

Fighting Noise with Noise: Causal Inference with Many Candidate Instruments

Xinyi Zhang, Linbo Wang, Stanislav Volgushev and Dehan Kong

University of Toronto, Department of Statistical Sciences

Abstract

Instrumental variable methods provide useful tools for inferring causal effects in the presence of unmeasured confounding. To apply these methods with large-scale data sets, a major challenge is to find valid instruments from a possibly large candidate set. In practice, most of the candidate instruments are often not relevant for studying a particular exposure of interest. Moreover, not all relevant candidate instruments are valid as they may directly influence the outcome of interest. In this article, we propose a data-driven method for causal inference with many candidate instruments that addresses these two challenges simultaneously. A key component of our proposal is a novel resampling method that constructs pseudo variables to remove irrelevant candidate instruments having spurious correlations with the exposure. Theoretical and synthetic data analyses show that the proposed method performs favourably compared to existing methods. We apply our method to a Mendelian randomization study estimating the effect of obesity on health-related quality of life.

Keywords: A/B tests; Mendelian randomization; Selection bias; Spurious Correlation

1 Introduction

The instrumental variable (IV) model is a workhorse in causal inference using observational data. It is especially useful when standard adjustment methods are biased due to unmeasured confounding. The key idea is to find an exogenous variable to extract random variation in the exposure and use this random variation to estimate the causal effect. This exogenous variable is known as the instrumental variable or instrument if it is related to the exposure, but does not affect the outcome directly except through the exposure.

In the past, the selection of appropriate exogenous variables that can serve as valid instruments is typically driven by expert knowledge (e.g. [Angrist & Krueger, 1991](#)). In recent years, applied researchers have increasingly sought to employ large-scale observational data sets to identify causal relationships. As the size and complexity of data sets grow, it becomes increasingly difficult to build a knowledge-based instrumental variable model for modern data applications. A prominent example in genetic epidemiology is Mendelian randomization (MR), which uses genetic variants, such as single-nucleotide polymorphisms (SNPs), as instruments to assess the causal relationship between a risk factor and an outcome (e.g. [Burgess et al., 2015](#)). The candidate instrument set includes millions of SNPs in the human genome. This challenge also arises in the literature using multi-condition experiments as instruments (e.g. [Eckles et al., 2016](#); [Goldman & Rao, 2016](#); [Peysakhovich & Eckles, 2018](#)). For example, in tech companies, it is common to have routine product experimentation such as A/B tests. These large collections of randomized experiments provide natural candidates for finding instrumental variables.

Modern large-scale complex systems call for data-driven methods that find valid instruments from a high-dimensional candidate set. Two main challenges arise from such a pursuit. First, often most of the candidate instruments are not relevant for studying a particular exposure of interest. To deal with this problem, a common procedure is to employ a screening procedure (e.g. [Fan & Lv, 2008](#)) to select variables in the candidate set that are associated with the exposure. For example, in genetics, it is common to use genome-wide association studies (GWAS) or variants thereof to identify genetic variants that are relevant to a risk factor. Recent studies have suggested choosing a less conservative selection threshold than the traditional 5×10^{-8} for MR applications (e.g. [Zhao et al., 2020](#)), in order to include more SNPs that are associated with the risk factors and hence improve the efficiency of the resulting causal effect estimate; see also [Barber & Candes \(2019\)](#) for a similar recommendation in a related context. This is especially important for datasets with small to moderate sample sizes, for which standard GWAS has limited power so that only very few or even no genetic variants may be selected. On the other hand, a less conservative selection threshold will result in more false positive, i.e. SNPs having spurious correlations with the risk factor of interest. Using these SNPs as instruments will undermine the validity of the downstream MR procedures. A similar problem also arises in multi-condition experiments as most of the experiments have very small effects on the exposure ([Peysakhovich & Eckles, 2018](#)).

Moreover, some of the candidate instruments found to be associated with the exposure might not be valid as they may directly influence the outcome of interest. For example, in MR studies, this problem arises due to pleiotropy, a phenomenon that one genetic variant influences multiple traits and possibly through independent pathways. In response to this concern, recently there has been a surging interest in methods that make valid causal inference in the presence of invalid instruments. [Kolesar et al. \(2015\)](#) and [Bowden et al. \(2015\)](#) provided inferential methods for treatment effects in the presence of invalid instruments. Their methods rely on a strong assumption that the direct effects of these invalid instruments are uncorrelated with the associations between the instruments and the exposure. Some others ([Bowden et al., 2016](#); [Burgess et al., 2016](#); [Kang et al., 2016](#); [Wind-](#)

meijer et al., 2019; Hartford et al., 2021) assumed that at least 50% of the candidate instruments are valid. This assumption, known as the “majority rule,” allows them to establish consistency and inferential guarantees. Relaxing the majority rule, Guo et al. (2018) and Windmeijer et al. (2021) assume that valid instruments appear most often, referred to as “plurality rule.” They also proposed two-stage thresholding procedures to identify valid IVs and consistently estimate causal effect. In the MR context, Morrison et al. (2020) proposed a method based on genome-wide summary statistics that accounts for both uncorrelated and correlated pleiotropic effects, while Zhao et al. (2020) proposed a consistent causal effect estimator by adjusting profile likelihood of the summary data under a two-sample MR design where the exposure and the outcome are observed from two independent samples.

Our developments in this paper are motivated by the somewhat surprising finding that a naive application of existing methods for solving the two challenges discussed above leads to biased causal inference. In many scenarios, estimates from this naive application are close to the ordinary least squares (OLS) estimate that does not account for any unmeasured confounding. Recall that when the sample size is small or moderate, there may be many false positives from the first screening step. Furthermore, using these false positives as instruments leads to similar estimates as the OLS. A related finding from the literature on weak IVs is that the bias of IV estimates approaches that of OLS estimates as the correlation between the instruments and exposure approaches zero (Nelson & Startz, 1990a; Bound et al., 1995; Stock et al., 2002). Related approaches to deal with weak IVs have been discussed in Donald & Newey (2001); Carrasco (2012); Carrasco & Tchuente (2015).

In this paper, we introduce a novel strategy that addresses these two challenges simultaneously. A key component of our proposal is a resampling method that constructs pseudo variables to identify and remove false positives. The idea of pseudo variables has been investigated before in other contexts, most notably in forward selection (Wu et al., 2007). It is also similar in spirit to knockoffs (Barber & Candès, 2015) although our construction of pseudo variables is much simpler and relies on fewer assumptions than the construction of knockoffs. We provide theoretical guarantees that the estimates from exogenous variables having spurious correlations with the exposure are concentrated in a region that is separated from the true causal effect. Hence our procedure can remove the false positives but retain the valid instruments. It is noteworthy that the concentration results we provide are conditional on a hard thresholding step that reduces the set of candidate instruments to a moderate size. As such, the tail bounds of interest depend on a random collection of candidate instruments. In this case, the independence assumptions required for standard concentration results fail to hold, and standard methods such as the Hoeffding bound, Bernstein-type inequalities or entropic methods are no longer directly applicable. We also show how to make valid inferences on the causal effect via sample splitting, in which one portion of the data is used to identify the false positives, and the remaining data are used to identify the valid instruments and estimate the causal effect. We establish asymptotic properties of the resulting causal effect estimator, building on which we construct valid confidence intervals for the causal effect of interest.

The rest of this article is organized as follows. In Section 2, we introduce our models and illustrate the challenges of finding valid instruments from a large candidate set using a simulated example. Section 3 details the proposed procedure. We provide theoretical justifications in Section 4. In Section 5, we evaluate the performance of our procedure via simulations. In Section 6, we apply the proposed method to the Wisconsin Longitudinal Study data and examine the causal effect of obesity on Health-Related Quality of Life (HRQL).

2 Background and Motivation

2.1 Instrumental variable methods

The instrumental variable (IV) approach is a popular method for inferring causality from observational studies. It introduces exogenous variables called instruments to control for unmeasured confounding U . Conditioning on observed covariates, a variable Z is called an IV for estimating the causal effect of an exposure D on an outcome Y if it satisfies the three core conditions (e.g. [Didelez & Sheehan, 2007](#); [Wang & Tchetgen Tchetgen, 2018](#)) below:

- I1 Relevance: Z is associated with the exposure;
- I2 Exclusion restriction: Z has no direct effect on the outcome;
- I3 Independence: Z is independent of unmeasured variables that affect the exposure and the outcome.

Figure 1 gives a causal graph representation of the IV model.

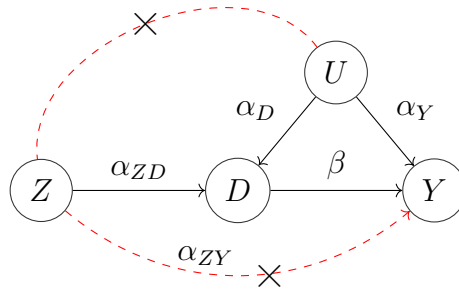


Figure 1: Graphical illustration of an IV model: Z denotes a valid instrument, D, Y represent the exposure and outcome, respectively and U is the unobserved confounding. Parameters on the arrows represent effects on the linear scale. Red dashed lines with \times indicate absence of arrows.

Suppose we observe n independent samples $(Y_i, D_i, \mathbf{Z}_i, \mathbf{X}_i)$ from the distribution of $(Y, D, \mathbf{Z}, \mathbf{X})$, where Y is a continuous outcome of interest, D is a continuous exposure, $\mathbf{Z} = (Z_1, \dots, Z_p)^T \in \mathbb{R}^p$

denotes candidate instrumental variables, and $\mathbf{X} = (X_1, \dots, X_q)^T \in \mathbb{R}^q$ represents baseline covariates. We assume that D and Y are generated from the following linear structural equation models:

$$D = \mathbf{Z}^T \boldsymbol{\gamma} + \mathbf{X}^T \boldsymbol{\psi} + \alpha_D U + \epsilon_D; \quad (2.1)$$

$$Y = \mathbf{Z}^T \boldsymbol{\pi} + \beta D + \mathbf{X}^T \boldsymbol{\phi} + \alpha_Y U + \epsilon_Y. \quad (2.2)$$

The parameter β measures the causal effect of the exposure D on the outcome Y , which is the estimand of our primary interest. Parameter $\boldsymbol{\gamma} \in \mathbb{R}^p$ characterizes the partial correlations between the instruments and the exposure. Parameter $\boldsymbol{\pi} \in \mathbb{R}^p$ measures the degree of violation of the exclusion restriction assumption I2. Parameters $\alpha_D \in \mathbb{R}$ and $\alpha_Y \in \mathbb{R}$ correspond to the direct effects of the univariate unobserved confounder U on the exposure and on the outcome, respectively. The assumption of univariate confounding here is made for ease of exposition and will later be relaxed in Section 4. Unmeasured confounding U and random errors ϵ_D, ϵ_Y are independently distributed with mean zero and variance $\sigma_U^2, \sigma_D^2, \sigma_Y^2$, respectively. We further assume that Z_j is independent of ϵ_D, ϵ_Y and U for $j = 1, \dots, p$. This assumption is generally considered plausible in MR studies after controlling for population stratification (Smith, 2007; Zhao et al., 2020) and holds by design in multi-condition experiments. The true parameter values of $\beta, \boldsymbol{\gamma}, \boldsymbol{\pi}, \alpha_D$ and α_Y are denoted by $\beta^*, \boldsymbol{\gamma}^*, \boldsymbol{\pi}^*, \alpha_D^*$ and α_Y^* respectively. An instrument Z_j is called relevant if $\gamma_j^* \neq 0$, and is called irrelevant otherwise. For relevant instruments, if $\pi_j^* = 0$, then Z_j is a valid instrument; otherwise, it is called an invalid instrument.

For the rest of the paper, we suppress dependence on covariates \mathbf{X} for simplicity. With this, models (2.1) and (2.2) take the reduced forms

$$D = \mathbf{Z}^T \boldsymbol{\gamma} + \alpha_D U + \epsilon_D, \quad (2.3)$$

$$Y = \mathbf{Z}^T \boldsymbol{\Gamma} + (\beta \alpha_D + \alpha_Y) U + e, \quad (2.4)$$

where $\boldsymbol{\Gamma} = \boldsymbol{\pi} + \beta \boldsymbol{\gamma}$ and $e = \beta \epsilon_D + \epsilon_Y$. Let $\mathbb{Z} \in \mathbb{R}^{n \times p}$, $\mathbf{D} \in \mathbb{R}^n$ and $\mathbf{Y} \in \mathbb{R}^n$ denote the collection of observations for (\mathbf{Z}, D, Y) from n units, respectively. Here \mathbb{Z} is also called the design matrix. Without loss of generality, assume that $\mathbb{Z}, \mathbf{D}, \mathbf{Y}$ are all centered.

Given a valid instrument Z_j , the causal effect β may be identified as the Wald ratio (Lawlor et al., 2008). Alternatively, given a set of valid instruments $\mathbf{Z}_{\text{valid}}$, a popular procedure to estimate the causal effect under linear models is the two-stage least squares (2SLS) estimator given by $\hat{\beta}_{2\text{SLS}} = (\mathbf{D}^T \mathbf{P} \mathbf{D})^{-1} (\mathbf{D}^T \mathbf{P} \mathbf{Y})$, where $\mathbf{P} = \mathbb{Z}_{\text{valid}} (\mathbb{Z}_{\text{valid}}^T \mathbb{Z}_{\text{valid}})^{-1} \mathbb{Z}_{\text{valid}}^T$ is a projection matrix and $\mathbb{Z}_{\text{valid}}$ is the design matrix of valid instruments.

In practice, prior knowledge of instrument validity is often not available. Nevertheless, the causal effect can still be identified and estimated from data under the majority rule that more than 50% of the candidate IVs are valid. In this case, among the Wald ratios constructed using individual candidate IVs, more than 50% of them equal the true causal effect β . As a result, β

can be identified as the median of these Wald ratios (e.g. Han, 2008; Bowden et al., 2016). The majority rule may be relaxed to the so-called plurality rule, which assumes that the largest group of invalid instruments with the same Wald ratio is smaller than the group of valid instruments, whose Wald ratio equals the true causal effect. In this case, the mode of the Wald ratios constructed using individual candidate IVs corresponds to the true causal effect (e.g. Guo et al., 2018; Windmeijer et al., 2021).

2.2 Challenges with high dimensional candidate instruments

The majority or plurality rule may be violated empirically if the dimension of candidate instruments is large relative to the sample size. We illustrate this problem using a simulated example. We generate 1000 data sets of size $n = 500$ with $p = 50,000$ candidate instruments. The true causal effect β^* is set to be 2. Candidate instruments Z_1, Z_2 are invalid, Z_3, \dots, Z_7 are valid, and $Z_8, \dots, Z_{50,000}$ are irrelevant. The valid instruments $\mathbf{Z}_{3:7} \sim N(\mathbf{0}, \Sigma_v)$ with $[\Sigma_v]_{jk} = 0.25^{|j-k|}$. The other candidate instruments $Z_j, j = 1, 2, 8, \dots, 50,000$, the observed covariates X_1, X_2 , the random error ϵ_Y , and the unobserved confounding U are generated from independent standard normal distributions. The treatment D and the outcome Y are generated following models (2.1) and (2.2), where $(\alpha_D^*, \alpha_Y^*) = (5, -2)$, the relevance strength $\gamma_{1:7}^* = 3$ and the degree of violation to the exclusion restriction assumption is characterized by $\pi_{1:2}^* = (-3.5, 3.5)^T$; the effects of the observed covariates on the exposure and the outcome are given by $\psi^* = (1.5, 2)^T$ and $\phi^* = (1.2, 1.5)^T$, respectively. For simplicity, we let $\epsilon_D = 0$.

As an illustration, we apply the two-stage hard thresholding (TSHT) with voting procedure (Guo et al., 2018) to identify valid IVs and estimate the causal effect. To make this computationally feasible, we first reduce the candidate set to a moderate size via a pre-screening step. Specifically, we marginally regress the exposure on each candidate instrument and keep the 500 with the largest marginal associations in absolute value. Empirical results suggest that most of the valid instruments identified by the TSHT with voting are in fact irrelevant. On average, the TSHT identifies 14.86 variables as valid IVs, among which 14.84 are in fact irrelevant. The empirical coverage probability constructed from the TSHT procedure is 7%, compared to a nominal level of 95%.

To provide insights into this problem, we study the candidate instruments Z'_j s that pass a selection step with regard to the exposure, referred to as joint thresholding by Guo et al. (2018). In Figure 2(a), we plot the histograms of causal effect estimates aggregated over the 1000 Monte Carlo runs. We use different colors to distinguish the estimates produced by the valid, invalid IVs and irrelevant variables. One can see that the plurality rule is violated empirically even after joint thresholding: compared to valid IVs, there are more candidate instruments having spurious correlations with the exposure left after joint thresholding. The latter variables shall be referred to as “spurious instruments.” The plurality rule is violated here because there are much more irrelevant “instruments” to begin with, and the sample size is small relative to the number of candidate instruments. Somewhat surprisingly, all spurious instruments lead to similar causal effect estimates.

Moreover, these effect estimates lie in a region that is separated from those estimates by the valid IVs. As a result, the TSHT with voting procedure that assumes the plurality rule misidentifies the spurious instruments as valid IVs, as shown in Figure 2(b).

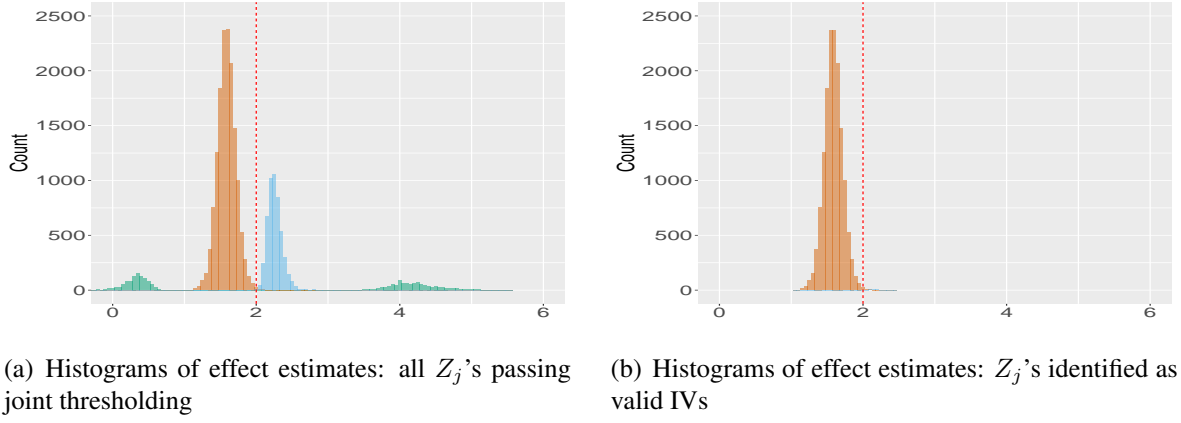


Figure 2: Histograms of causal effect estimates aggregated over the 1000 Monte Carlo runs: (a) plots the estimates by candidate instruments that pass the joint thresholding step of Guo et al. (2018), and (b) plots the estimates by candidate instruments identified as valid instruments using the method by Guo et al. (2018). The blue pile represents causal effect estimates by valid IVs; the green piles represent those by invalid IVs; the orange pile represents those by irrelevant variables. The red dashed line is the true causal effect $\beta^* = 2$.

The somewhat surprising behaviour of spurious instruments can be explained using the directed acyclic graph (DAG) in Figure 3. Suppose that candidate Z is irrelevant to D, Y but there is a

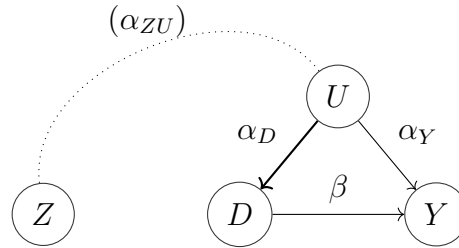


Figure 3: Black dotted line “.....” refers to sample correlation between Z and U . The thick arrow “ \longrightarrow ” represents that D is determined by U . α_D and α_Y are effects of U on D and Y respectively. (α_{ZU}) refers to spurious correlation between Z and U . β denotes the causal effect.

spurious pathway between Z and U . In other words, Z and U are independent in the population but the sample correlation between them, denoted by α_{ZU} , is non-zero by pure chance. Under linearity, the sample correlation between Z, D and Z, Y becomes $\alpha_D \alpha_{ZU}$ and $(\beta \alpha_D \alpha_{ZU} + \alpha_Y \alpha_{ZU})$, respectively. Taking ratio of the two correlations gives $\beta + \alpha_Y / \alpha_D$. Hence under this simple setting,

the bias of causal effect estimates by spurious instruments is concentrated at α_Y/α_D , which is the same as the bias of OLS estimate (Stock et al., 2002; Nelson & Startz, 1990b).

3 Fighting Noise with Noise

As illustrated in Section 2.2, a major challenge for causal inference with many candidate instruments is the identification of spurious instruments and distinguishing the valid instruments from the spurious ones. To solve this problem, the key idea in our developments is to add independent noises, known as pseudo variables, to the real data set. These pseudo variables mimic the behaviour of the irrelevant variables in the candidate instrument set, as both of them are independent of the exposure D .

Specifically, since the vast majority of candidate instruments in most applications are irrelevant, we propose to generate p pseudo variables Z_{p+1}, \dots, Z_{2p} by randomly permuting the rows of the design matrix $\mathbb{Z} \in \mathbb{R}^{n \times p}$. The resulting matrix \mathbb{Z}^* is independent of D , while keeping the correlation structure in the original candidate instruments \mathbf{Z} . The expanded candidate instrument matrix $\tilde{\mathbb{Z}} \in \mathbb{R}^{n \times 2p}$ is defined as the concatenation of \mathbb{Z} and \mathbb{Z}^* .

By definition, pseudo variables are irrelevant. So the models (2.1) and (2.2) still hold with $\mathbf{Z} \in \mathbb{R}^p$ replaced by $\tilde{\mathbf{Z}} \in \mathbb{R}^{2p}$. With slight abuse of notation, hereafter we still use $\gamma \in \mathbb{R}^{2p}$ to denote the coefficient of $\tilde{\mathbf{Z}}$ in the exposure model with $\gamma_j = 0$ for $j = p+1, \dots, 2p$, and similarly for the parameter Γ in the outcome model. Similar to Guo et al. (2018), to reduce the set of candidate instruments, we perform a joint thresholding step in which we fit the reduced form models (2.3) and (2.4) with the set $\tilde{\mathbf{Z}}$. We consider the high-dimensional regime in which the number of candidate instruments goes to infinity. The coefficients γ and Γ may be estimated using regularization approaches such as the de-biased lasso estimator (e.g. Javanmard & Montanari, 2014) defined as follows:

$$\begin{aligned}\hat{\Gamma} &= \tilde{\Gamma} + \frac{1}{n} \mathbf{M} \tilde{\mathbb{Z}}^T (\mathbf{Y} - \tilde{\mathbb{Z}} \tilde{\Gamma}), \\ \hat{\gamma} &= \tilde{\gamma} + \frac{1}{n} \mathbf{M} \tilde{\mathbb{Z}}^T (\mathbf{D} - \tilde{\mathbb{Z}} \tilde{\gamma}),\end{aligned}\tag{3.1}$$

where the lasso estimator $\tilde{\Gamma} = \arg\min_{\Gamma \in \mathbb{R}^{2p}} \{\|\mathbf{Y} - \tilde{\mathbb{Z}} \Gamma\|_2^2 / (2n) + \lambda \|\Gamma\|_1\}$, and the lasso estimator $\tilde{\gamma}$ is defined similarly. The rows of the matrix $\mathbf{M} = (\mathbf{m}_1, \dots, \mathbf{m}_{2p})^T \in \mathbb{R}^{2p \times 2p}$, in which $\mathbf{m}_j \in \mathbb{R}^{2p}$, are defined via the optimization problem below

$$\mathbf{m}_j \in \arg\min_{\mathbf{m} \in \mathbb{R}^{2p}} \mathbf{m}^T \hat{\Sigma} \mathbf{m} \quad \text{subject to } \|\hat{\Sigma} \mathbf{m} - e_j\|_\infty \leq \mu \text{ for } 1 \leq j \leq 2p,\tag{3.2}$$

where $e_j \in \mathbb{R}^{2p}$ is a unit vector with the j th element equal to one and zero otherwise, and $\hat{\Sigma} =$

Algorithm 1 Fighting noise with noise

INPUT: Design matrix $\mathbb{Z} \in \mathbb{R}^{n \times p}$, observed exposure $\mathbf{D} \in \mathbb{R}^n$, observed outcome $\mathbf{Y} \in \mathbb{R}^n$.

0. Pseudo variables generation:

Generate p pseudo variables Z_{p+1}, \dots, Z_{2p} by randomly permuting the rows of \mathbb{Z} ;

Denote the resulting design matrix as \mathbb{Z}^* , and the concatenation of \mathbb{Z} and \mathbb{Z}^* as $\tilde{\mathbb{Z}}$.

1. Joint thresholding:

Fit a linear model for $\mathbf{D} \sim \tilde{\mathbb{Z}}$: let $\hat{\gamma}$ be the debiased lasso estimate defined in (3.1). Also obtain their standard error estimate $\text{SE}(\hat{\gamma}_l)$ in (3.3).

Fit a linear model for $\mathbf{Y} \sim \tilde{\mathbb{Z}}$ and obtain the estimate $\hat{\Gamma}$ in a similar fashion.

Estimate the relevant variables $\hat{\mathcal{S}}_1 = \{1 \leq l \leq 2p : |\hat{\gamma}_l| \geq \delta_n \times \text{SE}(\hat{\gamma}_l)\}$, where $\delta_n = \sqrt{\omega \log(\max\{n, 2p\})}$ and ω is a tuning parameter. Denote pseudos in $\hat{\mathcal{S}}_1$ by $\hat{\mathcal{P}}$.

2. Irrelevant variables removal:

For each $l \in \hat{\mathcal{S}}_1$, calculate a causal effect estimate $\hat{\beta}^{(l)} = \hat{\Gamma}_l / \hat{\gamma}_l$;

Remove variables similar to pseudo variables in their causal effect estimate $\hat{\beta}^{(l)}$ from $\hat{\mathcal{S}}_1$:

$$\hat{\mathcal{S}}_2 = \hat{\mathcal{S}}_1 \setminus \left\{ l \in \hat{\mathcal{S}}_1 : \min_{j \in \hat{\mathcal{P}}} \hat{\beta}^{(j)} \leq \hat{\beta}^{(l)} \leq \max_{j \in \hat{\mathcal{P}}} \hat{\beta}^{(j)} \right\}.$$

3. Mode finding:

For $j, l \in \hat{\mathcal{S}}_2$, compute $\hat{b}^{(j,l)} = \hat{\beta}^{(l)} - \hat{\beta}^{(j)}$ and $\text{SE}(\hat{b}^{(j,l)})$;

For $j \in \hat{\mathcal{S}}_2$, find the number of candidates leading to a similar causal effect estimate with Z_j :

$$V_j = \left| \left\{ l \in \hat{\mathcal{S}}_2 : |\hat{b}^{(j,l)}| / \text{SE}(\hat{b}^{(j,l)}) \leq \sqrt{\omega^2 \log(\max\{n, 2p\})} \right\} \right|;$$

Find valid IVs using the plurality rule:

$$\hat{\mathcal{S}}_3 = \left\{ j : V_j = \max_{l \in \hat{\mathcal{S}}_2} V_l \right\}.$$

4. Causal effect estimation: Obtain 2SLS estimate for the causal effect with the IV set $\hat{\mathcal{S}}_3$.

$\tilde{\mathbf{Z}}^T \tilde{\mathbf{Z}}/n$. The standard error of the de-biased lasso estimate $\hat{\gamma}_l$ for $1 \leq l \leq 2p$ is given by

$$\text{SE}(\hat{\gamma}_l) = \sqrt{[\mathbf{M} \hat{\Sigma} \mathbf{M}^T/n]_{ll} \|\mathbf{D} - \tilde{\mathbf{Z}} \tilde{\gamma}\|^2/n}, \quad (3.3)$$

where $[\cdot]_{ll}$ denotes the l th diagonal element of the matrix. The hard thresholding step proceeds by comparing $|\hat{\gamma}_l|$ with a hard threshold $\delta_n \times \text{SE}(\hat{\gamma}_l)$, where $\delta_n = \sqrt{\omega \log(\max\{n, 2p\})}$ and ω is a tuning parameter that controls the number of candidates passing the joint thresholding (Donoho & Johnstone, 1994; Donoho, 1995). We use $\hat{\mathcal{S}}_1$ to denote the set of candidate instruments that pass this joint thresholding, that is, $\hat{\mathcal{S}}_1 = \{l : 1 \leq l \leq s, |\hat{\gamma}_l| \geq \delta_n \times \text{SE}(\hat{\gamma}_l)\}$.

Remark 3.1. The tuning parameter ω plays an important role in our procedure. As we shall demonstrate later theoretically, larger values for ω lead to better concentration of effect estimates from spurious instruments passing joint thresholding. At the same time, large values of ω mean that the joint thresholding step filters out more variables. In finite samples this can lead to discarding some valid instruments, leading to efficiency loss in the downstream analysis.

In Step 2 of Algorithm 1, we identify the spurious instruments and remove them from the candidate set, together with all the pseudo variables. Specifically, we calculate the ratio estimate $\hat{\beta}^{(l)} = \hat{\Gamma}_l/\hat{\gamma}_l$ for each $l \in \hat{\mathcal{S}}_1$. We then remove all the pseudo variables from $\hat{\mathcal{S}}_1$, together with all the candidate instruments whose corresponding causal effect estimate $\hat{\beta}^{(l)}$ falls into the range of causal effect estimates corresponding to the pseudo variables. The resulting set of candidate instruments is denoted as $\hat{\mathcal{S}}_2$.

In Step 3 of Algorithm 1, we develop a mode-finding algorithm to distinguish the valid instruments from the invalid and remaining spurious instruments. Similar to the literature on invalid IVs, we assume the plurality rule holds in $\hat{\mathcal{S}}_2$, i.e. the largest group of invalid or remaining spurious instruments with the same Wald ratio is smaller than the group of valid instruments. Recall that the mode is the value that appears most frequently in a data set. Hence

$$\text{mode}\{\beta^{(l)} : l \in \hat{\mathcal{S}}_2\} = \underset{\beta^{(l)} : l \in \hat{\mathcal{S}}_2}{\text{argmax}} |\{j \in \hat{\mathcal{S}}_2 : \beta^{(j)} = \beta^{(l)}\}|, \quad (3.4)$$

where $|\cdot|$ denotes cardinality of a set. To account for statistical uncertainty due to estimating $\beta^{(l)}$ in (3.4), we say two estimates $\hat{\beta}^{(j)}$ and $\hat{\beta}^{(l)}$ are close if $|\hat{b}^{(j,l)}|/\text{SE}(\hat{b}^{(j,l)})$ is below a certain threshold; here $\hat{b}^{(j,l)} = \hat{\beta}^{(l)} - \hat{\beta}^{(j)}$ is the distance between the estimates $\hat{\beta}^{(j)}$ and $\hat{\beta}^{(l)}$, and we discuss derivation of $\text{SE}(\hat{b}^{(j,l)})$ in the supplementary materials. Following Donoho & Johnstone (1994), we recommend $\sqrt{\omega^2 \log(\max\{n, 2p\})}$ as the threshold. Here we use ω^2 because of the number of pairwise comparisons. The mode in (3.4) is then estimated to be the effect estimate $\hat{\beta}^{(l)}$ that is close to the other estimates most frequently. Our estimated set of valid IVs $\hat{\mathcal{S}}_3$ consists of all candidate instruments whose corresponding causal effect estimates are close to the mode.

Once we have identified the set of valid IVs, it is straightforward to estimate the causal effect using two-stage least squares. This is summarized in Step 4 of Algorithm 1.

Remark 3.2. The voting algorithm implemented in Section 2.2, originally developed by Guo et al. (2018), uses a different approach than our Step 3 in Algorithm 1. It treats each of the candidate instrument $Z_l, l \in \hat{\mathcal{S}}_2$ as an expert, and each expert cast votes for other $Z_j, j \in \hat{\mathcal{S}}_2$. Importantly, this voting algorithm is not symmetric in that expert l casting vote for j does not imply expert j casting vote for l . In fact, under their algorithm, an effect estimate with a larger variance is likely to receive more votes. This is undesirable as the effect estimates with larger variances likely come from weak or spurious IVs. Our procedure above solves this problem under our setting.

Remark 3.3. If the dimension of candidate instruments p is large, then the debiased lasso in Step 1 of Algorithm 1 can be computationally challenging. To deal with this problem, it is common to first apply a preprocessing step to screen out variables that are unlikely to be relevant to the exposure (e.g. Fan & Lv, 2008). For our numerical experiments and data analysis, we rank the candidate instruments by their absolute marginal correlations with the exposure, and keep the top ones.

4 Theoretical Results

4.1 Separation between the spurious and valid instruments

In this part, we provide theoretical support for the empirical finding in Section 2.2 that causal effect estimates from spurious instruments are separable from those estimates produced by valid instruments. In particular, we show that the estimates from spurious instruments that pass the joint thresholding step concentrate in an interval $[\beta^* + C_* - d, \beta^* + C_* + d]$, where $C_* = (\alpha_Y^* \alpha_D^* \sigma_u^2) / (\alpha_D^{*2} \sigma_u^2 + \sigma_D^2)$, and d depends on the variance terms $\alpha_D^{*2} \sigma_u^2$ and σ_D^2 . The estimates from valid instruments are centered around the true causal effect β^* . If d is small enough such that $d < |C_*|$, then the estimates produced by the spurious instruments are separable from the estimates produced by the valid instruments. As discussed in detail later, this happens when the confounding between D and Y is strong enough. In this case, it is possible to remove spurious instruments with the proposed method in Algorithm 1.

Results from the weak IV literature (Nelson & Startz, 1990b; Bound et al., 1995; Stock et al., 2002) suggest that as the instrumental strength approaches zero, the causal effect estimate approaches $\beta^* + C_*$. These results, however, assume that the number of weak instruments is fixed or increases at a slower rate than the sample size. Moreover, they place additional constraints on the rate of convergence of the relevance strength of weak IVs. In contrast, we allow the number of irrelevant candidate instruments to grow at an exponential rate.

Compared to standard concentration results such as the Hoeffding, Bernstein-type inequalities and entropic methods, proofs of Theorems 4.2 and 4.3 below are more challenging because these results are conditional on the random set $\hat{\mathcal{S}}_1$ of relevant/irrelevant variables that pass the joint thresholding step. In particular, the observations are no longer independent conditional on $\hat{\mathcal{S}}_1$,

while the independence assumption is key to standard concentration results in the literature.

Before introducing our concentration bounds, we define the sets of relevant and irrelevant variables

$$\begin{aligned}\mathcal{R} &= \{l : 1 \leq l \leq p, \gamma_l^* \neq 0\}, \\ \mathcal{I} &= \{l : 1 \leq l \leq p, \gamma_l^* = 0\}.\end{aligned}$$

The assumptions imposed to establish the theoretical results are presented in the following:

A1. U_i 's are *i.i.d.* $N(0, \sigma_u^2)$, ϵ_{iD} 's are *i.i.d.* $N(0, \sigma_D^2)$ and ϵ_{iY} 's are *i.i.d.* $N(0, \sigma_Y^2)$. Random errors $\epsilon_{iD}, \epsilon_{iY}$ and unobserved confounding U_i are mutually independent for $i = 1, \dots, n$. Moreover, $U_i, \epsilon_{iD}, \epsilon_{iY}$ are all independent of Z_{ij} for $1 \leq i \leq n$ and $1 \leq j \leq p$.

A2. Let $\Sigma \in \mathbb{R}^{p \times p}$ be the covariance matrix of $\mathbf{Z} \in \mathbb{R}^p$. There exist constants $C_L, C_R, B > 0$ such that for all p , $\lambda_{\min}(\Sigma) \geq C_L > 0$, $\lambda_{\max}(\Sigma) \leq C_R < \infty$, and $\max_{1 \leq j \leq p} \Sigma_{jj} \leq B$. Further assume \mathbf{Z} have *i.i.d.* sub-gaussian rows with variance proxy σ^2 and zero mean, i.e., for any $\lambda \in \mathbb{R}$ and unit vector $\mathbf{u} \in \mathcal{S}^{p-1}$, $E \left\{ e^{\lambda \mathbf{u}^T (\Sigma^{-1/2} \mathbf{Z}_1)} \right\} \leq e^{\frac{\sigma^2 \lambda^2}{2}}$, where \mathcal{S}^{p-1} is an Euclidean unit sphere in \mathbb{R}^p . We denote by $\kappa = \|\Sigma^{-1/2} \mathbf{Z}_1\|_{\psi_2}$ the sub-Gaussian norm of $\Sigma^{-1/2} \mathbf{Z}_i$ for $i = 1, \dots, n$, where κ is a finite positive constant.

A3. Irrelevant variables are irrelevant to both the exposure and the outcome, and are independent of relevant instruments.

A4. The size of relevant variables to the exposure D , $s_1^* = |\mathcal{R}|$, is fixed. We use s_2^* to denote the number of invalid instruments that violate the exclusion restriction assumption (I2).

A5. For some constant $c_0, C_0 > 0$, $c_0 \leq |\gamma_k^*| \leq C_0$ for all $k \in \mathcal{R}$. For invalid instrument $k \in \mathcal{I}$, the degree of violation satisfies $\check{c}_0 \leq |\pi_k^*| \leq \check{C}_0$ for some $\check{c}_0, \check{C}_0 > 0$.

Remark 4.1. A1 and A2 are distribution assumptions for candidate instruments, the unmeasured confounding and the random noise in the models (2.1) and (2.2). The Gaussian assumption on $\epsilon_Y, \epsilon_D, U$ is at a cost of additional technical complexity. If candidates are irrelevant to the exposure but correlated with the outcome, then we can treat them similarly to invalid instruments. Here we assume that irrelevant variables are irrelevant to both the exposure and outcome for the sake of simplicity, as presented in A3. The assumption A4 places sparsity level for the models. The relevance strength for valid and invalid instruments is provided in A5.

Theorem 4.2 gives the concentration statement about spurious instruments that pass the joint thresholding step, i.e., $\mathcal{I} \cap \hat{\mathcal{S}}_1$.

Theorem 4.2 (Concentration results for all spurious instruments). Suppose assumptions A1-A4 hold. Further assume $\log p = O(n^{\tau_1})$ for $0 < \tau_1 < 1$ and $p \rightarrow \infty$. Let $\mu = a_1 \sqrt{(\log p)/n}$

and $\lambda_\gamma = C_\gamma \sqrt{(\log p)/n}$, $\lambda_\Gamma = C_\Gamma \sqrt{(\log p)/n}$ for some constants $a_1 > 4\sqrt{3}e(C_R/C_L)^{1/2}\kappa^2$, $C_\gamma \geq 10\sqrt{B(\alpha_D^{*2}\sigma_u^2 + \sigma_D^2)}$, $C_\Gamma \geq 10\sqrt{B(\alpha_Y^{*2}\sigma_u^2 + \sigma_Y^2)}$, where $\mu, \lambda_\gamma, \lambda_\Gamma$ are tuning parameters in the optimization (3.2) and lasso problems respectively. If

$$d > \frac{1}{\sqrt{\omega}} \max \left\{ \frac{12|\alpha_Y^*|\sigma_u\sigma_D}{(\alpha_D^{*2}\sigma_u^2 + \sigma_D^2)}, \frac{6\sigma_Y}{\sqrt{(\alpha_D^{*2}\sigma_u^2 + \sigma_D^2)}} \right\},$$

then there exists a constant $\tilde{C}_4 = \tilde{C}_4(d) > 0$ such that

$$P\left(\max_{l \in \mathcal{I} \cap \hat{\mathcal{S}}_1} \left| \frac{\hat{\Gamma}_l}{\hat{\gamma}_l} - \beta^* - C_* \right| \leq d\right) \geq 1 - e^{-\tilde{C}_4 \log\{\min(p, n)\}}.$$

Next we show that causal effect estimates from valid IVs concentrate around the true causal effect β^* , and causal effect estimates from invalid IVs which violate the exclusion restriction assumption (I2) concentrate around $\beta^* + \pi_l^*/\gamma_l^*$, with $\pi_l^* \neq 0$ for $l \in \mathcal{R} \cap \hat{\mathcal{S}}_1$.

Theorem 4.3 (Concentration results for all relevant (valid and invalid) instruments). Suppose assumptions A1, A2 and A4, A5 hold. Further assume $\log p = O(n^{\tau_1})$ for $0 < \tau_1 < 1$ and $n = O(p)$. Under the same conditions on $\mu, \lambda_\gamma, \lambda_\Gamma$ as in Theorem 4.2, then there exist constants $c_6, \tilde{C}_5 > 0$ such that the following holds

$$P\left(\max_{l \in \mathcal{R} \cap \hat{\mathcal{S}}_1} \left| \frac{\hat{\Gamma}_l}{\hat{\gamma}_l} - \left(\beta^* + \frac{\pi_l^*}{\gamma_l^*}\right) \right| \leq c_6 \sqrt{\frac{\log p}{n}}\right) \geq 1 - e^{-\tilde{C}_5 \log p}.$$

Combining the findings in Theorem 4.2 and Theorem 4.3 shows that, for sufficiently large ω , the estimates from valid instruments are separated from those from spurious instruments with probability going to one. Indeed, from Theorem 4.3 we see that causal estimates from all valid instruments will concentrate around the true effect β^* . In contrast, estimates from spurious instruments concentrate within the interval $[\beta^* - C_* - d, \beta^* - C_* + d]$. This interval does not contain β^* provided that $|C_*| < d$, which can always be achieved by choosing ω sufficiently large.

The concentration results here can be generalized to accommodate a multivariate U with fixed dimension. In this case, the $\alpha_D U, \alpha_Y U$ in models (2.1) and (2.2) become $U^T \alpha_D$ and $U^T \alpha_Y$ respectively, and all the other terms remain the same. Let α_D^*, α_Y^* denote the true values of α_D, α_Y . If α_Y^* is orthogonal to α_D^* , i.e., $\alpha_Y^{*T} \alpha_D^* = 0$, then there is no confounding and the causal effect can be identified as the association between D and Y . If α_D^* is parallel to α_Y^* , that is, there exists a constant $a \neq 0$ such that $\alpha_Y^* = a\alpha_D^*$, then we can define $\tilde{U} = \alpha_D^{*T} U$ and $\alpha_Y^{*T} U$ can be rewritten as $a\tilde{U}$. Clearly, now it is reduced to the univariate setting. We defer detailed discussion to the supplementary materials.

4.2 Inference with sample splitting

Algorithm 1 plays a key role in removing most irrelevant variables, but can introduce selection bias into causal effect estimate. A classical approach to deal with selection bias is sample splitting. Below, we discuss how sample splitting can be implemented in the present context. Divide data into two halves: H_1 of size n_1 and H_2 of size n_2 . The first subsample is used to identify and remove the irrelevant variables, corresponding to Steps 0–2 of Algorithm 1. On the second subsample, we apply an additional joint thresholding step to further estimate relevant variables to the exposure. Then we use the proposed mode finding algorithm in Step 3 of Algorithm 1 to identify the valid instruments and estimate the causal effects. The resulting estimator is denoted by $\hat{\beta}_{\text{split}}$. These steps are summarized in Algorithm S1, with details discussed in Section S1, both in the supplementary materials.

To accommodate the plurality rule that valid instruments appear most often at population level with the estimation procedure, we introduce the empirical plurality rule that is necessary to establish the asymptotic results. Let $\mathcal{V}_* = \{1 \leq l \leq p : \gamma_l^* \neq 0 \text{ and } \pi_l^* = 0\}$ denote the set of valid instruments.

Definition 4.4. The empirical plurality rule holds if

$$|\mathcal{V}_*| > \max_{c \neq 0} |\{l \in \hat{\mathcal{S}}_2 : \pi_l^*/\gamma_l^* = c, \gamma_l^* \neq 0\}| \quad (\text{EPR}).$$

Theorem 4.5 summarizes the asymptotic properties of $\hat{\beta}_{\text{split}}$.

Theorem 4.5. Suppose that assumptions A1, A2 and A4, A5 hold, and $n_1 = cn_2$ for $c > 0$. Under the empirical plurality rule (EPR), we have

$$\sqrt{n_2}(\hat{\beta}_{\text{split}} - \beta) \xrightarrow{d} N\left(0, \frac{\alpha_Y^{*2}\sigma_u^2 + \sigma_Y^2}{v_{\text{split}}}\right) \quad (4.1)$$

as $n \rightarrow \infty$. Moreover,

$$P\left(\hat{\beta}_{\text{split}} - z_{1-\alpha/2}\sqrt{\hat{v}_{\text{split}}/n_2} \leq \beta \leq \hat{\beta}_{\text{split}} + z_{1-\alpha/2}\sqrt{\hat{v}_{\text{split}}/n_2}\right) \rightarrow 1 - \alpha \quad (4.2)$$

as $n \rightarrow \infty$, where $z_{1-\alpha/2}$ is the $(1 - \alpha/2)$ -quantile of the standard normal distribution. Details of v_{split} , \hat{v}_{split} are provided in (S1.3) and (S1.4) of the supplementary materials.

Remark 4.6. Although sample splitting can deal with selection bias in theory, it results in smaller samples used for identifying valid instruments and in the final estimation step. This can result in reduced efficiency and imprecise inference in smaller samples, which can overweight the positive effect of removing selection bias. We observe this effect in some of our simulations reported in Section 5.

5 Simulation Studies

In this section, we run numerical experiments to evaluate the performance of the proposed methods. The simulation setting here is the same as that in the motivating example in Section 2.2, except that here we consider various values of the random error variance in the exposure $\sigma_D^2 = 0, 4, 8$. We include the following methods for comparison:

- “Proposed” represents our proposed method in Algorithm 1. The lasso penalization parameter λ is chosen by five-fold cross validation and we take $\omega = 2.01$ (Donoho & Johnstone, 1994; Donoho, 1995).
- “Sample Splitting” refers to the sample splitting method outlined in Section 4.2 and detailed in Algorithm S1 of the supplementary materials. We choose $n_1 = 300$ and $n_2 = 200$.
- “TSHT” is the two-stage hard thresholding with voting procedure (Guo et al., 2018). The tuning parameters are chosen in the same way as “Proposed.”
- “Oracle” is the 2SLS estimator based on valid instruments only, which provides a benchmark for comparison.

Motivated by Remark 3.3 and the data application in Section 6, before implementing the methods “Proposed”, “Sample Splitting” and “TSHT”, we first apply a pre-screening step to reduce the dimension and keep the top 500 candidate instruments with the largest marginal correlation with the exposure in absolute value. We measure the performance through 1000 Monte Carlo simulations. Simulation results regarding estimated bias, root-mean-square error (RMSE) and empirical coverage are summarized in Table 1.

The simulation results suggest that the proposed procedure outperforms competing methods in terms of bias, efficiency and validity of inference. Similar to our findings in Section 2.2, estimates by TSHT are biased. Although sample splitting gives desired empirical coverage when σ_D^2 is small, the bias and RMSE are much larger compared to the ones obtained by the proposed method. When the variance of the random error in the exposure ϵ_D increases, the performance of the proposed method remains similar, which indicates that our approach works even when the variance of unobserved confounding is relatively small compared to that of the random error ϵ_D . For the sample splitting method, one can see the RMSE increases and the coverage probability decreases further below the nominal level when ϵ_D increases.

To better understand the performance of various methods as summarized in Table 1, we report the average number of valid, invalid and spurious instruments in \hat{S}_1 , \hat{S}_2 and \hat{S}_3 respectively in Table 2. The results show that TSHT would misidentify irrelevant variables as valid and miss many or even all the valid instruments. The sample splitting procedure can find most valid instruments and meanwhile remove most invalid and spurious instruments when the variance σ_D^2 is small. However, the estimated set of valid instruments will include some invalid ones as σ_D^2 increases since we

Table 1: Performance summary for various methods and σ_D^2 across 1000 Monte Carlo runs with $n = 500$ and $p = 50,000$. We make the numbers bold for the method with the best performance except for the oracle estimate. Standard errors are presented in the bracket if applicable. For simplicity, we write $SE = 0.00$ if $SE < 0.005$

	Method	Bias $\times 10$ (SE $\times 10$)	RMSE $\times 10$	Coverage (Nominal = 95%)
$\sigma_D^2 = 0$	Proposed	-0.13(0.02)	0.55	0.92
	Sample Splitting	-0.20(0.05)	1.44	0.95
	TSHT	-1.78(0.02)	1.85	0.07
	Oracle	-0.02(0.01)	0.30	0.95
$\sigma_D^2 = 4$	Proposed	-0.12(0.02)	0.71	0.92
	Sample Splitting	-0.19(0.05)	1.66	0.91
	TSHT	-1.37(0.02)	1.48	0.13
	Oracle	-0.02(0.01)	0.30	0.94
$\sigma_D^2 = 8$	Proposed	-0.08(0.02)	0.57	0.93
	Sample Splitting	-0.16(0.06)	2.00	0.86
	TSHT	-0.95(0.02)	1.06	0.26
	Oracle	-0.02(0.01)	0.30	0.94

Table 2: Average number of invalid, valid IVs and irrelevant variables in $\hat{\mathcal{S}}_1$ (the candidate set after joint thresholding), $\hat{\mathcal{S}}_2$ (the candidate set after removing spurious instruments) and $\hat{\mathcal{S}}_3$ (the estimated set of valid IVs), respectively. The results are based on $n = 500$, $p = 50,000$ and 1000 Monte Carlo runs. “—” stands for “inapplicable”

		$\hat{\mathcal{S}}_1$			$\hat{\mathcal{S}}_2$			$\hat{\mathcal{S}}_3$		
	Method	Invalid	Valid	Irrelevant	Invalid	Valid	Irrelevant	Invalid	Valid	Irrelevant
$\sigma_D^2 = 0$	Proposed	2.00	5.00	17.34	2.00	5.00	2.05	0.00	4.30	0.58
	Sample Splitting	1.94	4.98	19.34	1.94	4.83	1.88	0.06	4.79	0.03
	TSHT	2.00	5.00	14.85	—	—	—	0.00	0.02	14.84
$\sigma_D^2 = 4$	Proposed	2.00	5.00	20.10	2.00	4.98	2.03	0.00	4.18	0.58
	Sample Splitting	1.92	4.96	23.03	1.92	4.62	1.83	0.10	4.48	0.03
	TSHT	2.00	5.00	17.33	—	—	—	0.00	0.52	17.32
$\sigma_D^2 = 8$	Proposed	1.99	4.99	22.76	1.99	4.95	1.95	0.00	4.31	0.80
	Sample Splitting	1.89	4.92	26.35	1.89	4.18	1.86	0.17	3.90	0.05
	TSHT	2.00	5.00	19.85	—	—	—	0.00	1.61	19.84

only use part of the data and the estimates have larger variation than those obtained using the full sample. Consequently, the resulting causal effect estimate has moderate bias and the empirical coverage deviates from the nominal level. In comparison, our proposed method can locate spurious instruments with the help of pseudo variables and correctly identify most valid instruments even if σ_D^2 is large.

To provide further insights, we plot the distribution of $\hat{\beta}^{(j)}$ collected from all Monte Carlo runs for valid, invalid and spurious instruments in \hat{S}_1 , \hat{S}_2 and \hat{S}_3 respectively in (a)-(c) of Figure 4, obtained from the proposed method under $\sigma_D^2 = 0$. We can see that causal effect estimates from spurious instruments and valid instruments are separable. Most spurious instruments lie in the region formed by causal effect estimates from pseudo variables, and thus are removed by following the proposed procedure. Thereafter the collection of valid instruments satisfies the empirical plurality rule (EPR), so the following mode-finding algorithm is able to identify the valid instruments.

To further evaluate the performance of the proposed method, we consider other approaches and a variety of additional settings in Section S4 of the supplementary materials. In particular, in addition to the aforementioned competing methods, we demonstrate the superiority of our new mode-finding step compared to the one proposed in Guo et al. (2018) by comparing with the approach that replaces the mode-finding step in our procedure with the voting proposed in Guo et al. (2018). Moreover, we consider the scenario that irrelevant variables can be correlated with valid instruments. We also carry out numerical experiments, in which the “independence” IV assumption (I3) is violated. Furthermore, since irrelevant variable can be seen as an extreme case of the weak instrument, we compare with competing methods (Donald & Newey, 2001; Carrasco, 2012; Carrasco & Tchuente, 2015) in the econometric literature that deal with weak IVs.

6 Real Data Application

We apply the proposed procedure to evaluate the effect of obesity on Health-Related Quality of Life (HRQL). Obesity increases the risks of many health problems, such as heart disease, diabetes, high blood pressure, certain cancers. Mechanical stress resulting from obesity can also impair mental well-being (Myers & Rosen, 1999; Katz et al., 2000). Health-related quality of life (HRQL) is emerging as an important outcome in obesity studies, which refers to the overall effects of medical conditions on physical and mental functioning and well-being as subjectively evaluated and reported by the patient (Fontaine et al., 1996). The development of standardized measures of HRQL helps us better understand the impact of a given illness on physical and mental health, and further influences public health policies.

To examine the causal relationship between obesity and HRQL, we use data from the Wisconsin Longitudinal Study (WLS). Study participants were graduates from Wisconsin high schools in 1957 and their siblings (Herd et al., 2014). Survey data were collected from the original respondents or their parents in 1957, 1964, 1975, 1992, 2004, and 2011. Our analysis focuses on

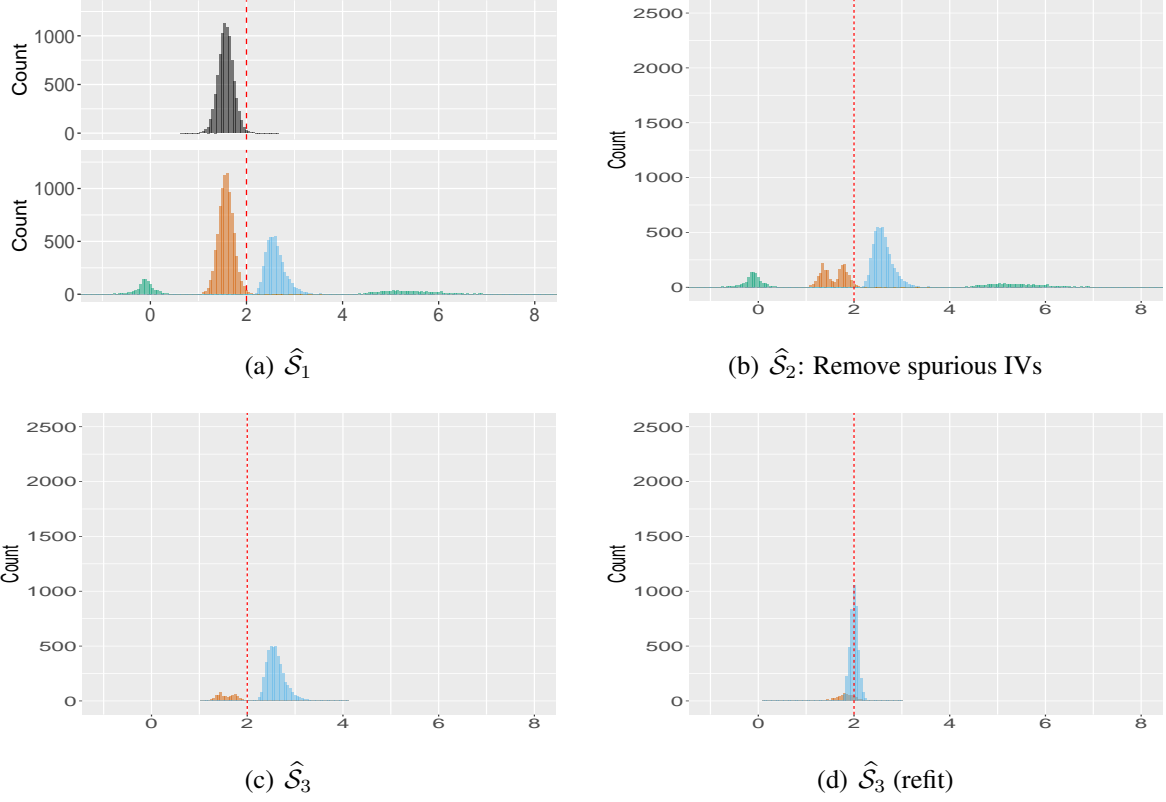


Figure 4: Plots (a)-(d) correspond to the simulation in Section 5: Plots (a) to (c) are histograms of causal effect estimates from valid, invalid and spurious instruments in $\hat{\mathcal{S}}_1$, $\hat{\mathcal{S}}_2$ and $\hat{\mathcal{S}}_3$ respectively obtained from Algorithm 1 across 1000 Monte Carlo runs. The blue pile represents causal effect estimates by valid IVs; the green piles represent those by invalid IVs; the orange pile represents those by irrelevant variables in the initial candidate set; the black pile represents those by pseudo variables. The red dashed line is the true causal effect $\beta^* = 2$. The results are based on $(n, p, \sigma_D^2) = (500, 50, 000, 0)$. Plot (d) gives the distribution of effect estimates from refitted model.

unrelated graduates reinterviewed in 2011. We take BMI as the exposure, a measure commonly used to define obesity. It ranges from 12 to 64 in the data set. The healthy range for BMI is between 18.5 and 24.9. As shown in Figure S1 in the supplementary materials, for underweight and normal individuals, HRQL is positively correlated with BMI, while for overweight or obese ones, HRQL is negatively correlated with BMI. Motivated by this observation, We shall restrict our analysis to participants whose BMI is above 25. There are 3023 subjects in total, 51% of which are females. In our analysis, the average BMI is 30.6 with standard deviation 4.93. To measure HRQL, we use the Health Utility Index Mark 3 (HUI-3) which takes values between -0.22 and 1. HUI-3 measured on the subjects in our analysis has mean 0.786 and standard deviation 0.227. We adjust for observed covariates including age, gender and year of education. Among participants considered in our analysis, the average age is 71.2 years old with standard deviation 0.9; the average education length is 13.8 years with standard deviation 2.38. We also adjust for the top six principal components to account for population stratification (Patterson et al., 2006; Sanderson et al., 2021), which are obtained by performing principal components analysis (PCA) on unrelated study participants.

We begin with a crude analysis that ignores the unmeasured confounding. Simply regressing the HUI-3 on BMI gives the OLS estimate -0.011 with 95% CI $[-0.013, -0.009]$. However, unmeasured factors such as smoking status and the use of alcohol may confound the relationship between BMI and HUI-3. In response to this potential problem, we use the MR method to investigate the causal relationship between these two. After quality control (QC) filtering of SNPs, we get a candidate set of 3,683,868 genetic variants in our MR analysis. Details of the QC steps are discussed in Section S2.3 of the supplementary materials. Following Algorithm 1, we generate pseudo variables by randomly permuting the SNP design matrix by rows, resulting in a candidate set of 7,367,736 variants in total.

We first apply a pre-screening step to quickly reduce the dimension of initial candidate instruments via ranking the marginal correlation in absolute value between each candidate instrument and the exposure. A common choice is to keep $\lfloor n/\log(n) \rfloor$ candidates (Fan & Lv, 2008), which is approximately 460 in our analysis. We round it to the nearest multiple of 100. Specifically, in the marginal screening step, by ranking the absolute marginal strength of association with BMI, we keep the top 500 candidate instruments. There were 261 true variants and 239 pseudo ones included in this set. To further identify genetic variants related to BMI, we fit a joint model for the 500 candidate instruments.

We visualize in Figure 5(a) the result from our proposed method. Specifically, a total of 86 SNPs ($\hat{\mathcal{S}}_1(\text{Proposed})$) pass the joint thresholding, corresponding to all the points shown in Figure 5(a). The 44 points on the left of the orange dashed line correspond to true genetic variants, while the 42 red dots on the right correspond to pseudo variants. In $\hat{\mathcal{S}}_1(\text{Proposed})$, causal effect estimates from 81 SNPs fall into the region formed by pseudo variants, which is represented by the band between the two black dashed lines. These SNPs are estimated as spurious and are removed from the candidate set. The remaining 5 points outside the region are genetic variants that are estimated to be relevant to BMI ($\hat{\mathcal{S}}_2(\text{Proposed})$). An application of the proposed mode-finding

procedure on $\hat{\mathcal{S}}_2(\text{Proposed})$ gives us 4 valid instruments ($\hat{\mathcal{S}}_3(\text{Proposed})$), corresponding to the blue squares in Figure 5(a): “rs199725608” on chromosome 1; “rs144468788” on chromosome 2 and in the MIR4432 host gene (MIR4432HG); “rs113116137” and “rs2546230” on chromosome 8, and “rs113116137” is in the CUB And Sushi Multiple Domains 1 (CSMD1) gene. The purple point at the bottom represents the estimated invalid instrument. Finally, we fit two-stage least squares using the four identified valid IVs and obtain the causal effect estimate $\hat{\beta} = -0.039$ with 95% confidence interval $[-0.051, -0.027]$. This suggests that in the overweight or obese population, one unit increase in BMI will result in 0.039 unit decrease of HUI-3.

To explore that the standard GWAS threshold might be too stringent to retain genetic variants associated with the trait of interest in our data application, we apply the genome-wide significance p -value threshold of 5×10^{-8} to the true genetic variants to identify significant associations with BMI. This gives us only one SNP “rs148605555” on chromosome 9. Although the SNP is estimated as relevant to BMI using our procedure, that is, the SNP is in the set $\hat{\mathcal{S}}_1(\text{Proposed})$, the associated effect estimate given by -0.011 lies in the middle of the estimated range by pseudos and thus the SNP is identified as spurious in the proposed method. In addition, the effect estimate of the SNP that passes the GWAS threshold is approximately the same as the OLS estimate, an indication that this might be a spurious one.

For comparison, we also apply the two-stage hard thresholding (TSHT) with voting (Guo et al., 2018) to this data set. The results are visualized in Figure 5(b). Specifically, we apply marginal screening to the true genetic variants only and keep the top 500 ($\mathcal{S}_1(\text{TSHT})$) by ranking absolute marginal strength concerning the exposure. Their joint thresholding step keeps 53 variants ($\hat{\mathcal{S}}_1(\text{TSHT})$), and the second stage of voting identifies 33 valid IVs ($\hat{\mathcal{S}}_3(\text{TSHT})$). Comparing the candidate instruments retained after the joint thresholding, we note that $\hat{\mathcal{S}}_1(\text{Proposed})$ and $\hat{\mathcal{S}}_1(\text{TSHT})$ have 19 variants in common. However, all these common SNPs are identified as irrelevant using our method. That is, $\hat{\mathcal{S}}_1(\text{TSHT}) \cap \hat{\mathcal{S}}_2(\text{Proposed}) = \emptyset$. This suggests that the TSHT with voting procedure might misidentify spurious instruments as valid IVs. Interestingly, the resulting causal effect estimate by TSHT with voting, that is -0.008 (95% CI $[-0.013, -0.003]$), is close to the OLS estimate.

To further understand the behaviour of TSHT with voting with this data set, we apply this method to the candidate set $\mathcal{S}_1(\text{Proposed})$ obtained after pre-screening in our procedure. In doing this, we pretend that the analyst does not know which variables in $\mathcal{S}_1(\text{Proposed})$ are pseudo variables. Analysis results in Figure 5(c) show that as expected, the TSHT with voting method misidentifies many pseudo variables as valid instruments. The resulting causal effect estimate, -0.013 (95% CI $[-0.016, -0.009]$), is also close to the OLS estimate.

In our data application, we did not implement the sample splitting Algorithm S1 for two main reasons: for one thing, the sample splitting method suffers from power loss, which is also demonstrated in our numerical experiments. And for another, the SNP matrix is encoded as 0,1,2, which represents possible genotypes. Splitting the data might dramatically change the genotype distribution since possibly some genotypes appear more often in one portion of the data but not the other

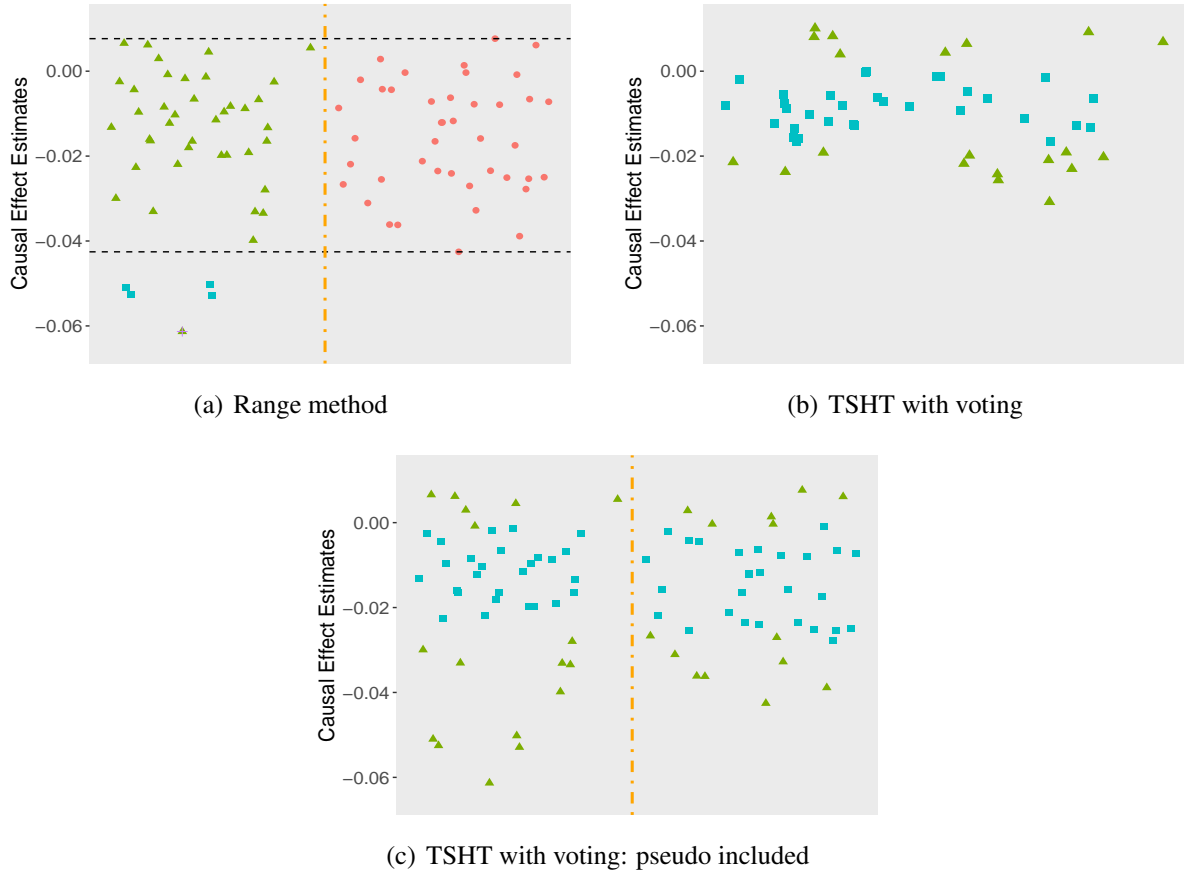


Figure 5: Causal effect estimates from estimated relevant SNPs versus SNP index. (a): Causal effect estimates associated with genetic variants in $\hat{S}_1(\text{Proposed})$. The orange dot-dashed line separates pseudo and real genetic variants. Red dots represent pseudo SNPs and all the others are true genetic variants. The two black dashed lines represent the estimated range. The four blue squares represented valid instruments identified through our procedure, and the gray diamond represents the invalid instrument we identified. (b): Causal effect estimates from relevant SNPs estimated by TSHT with voting procedure (Guo et al., 2018) which is applied to true variants only. The blue squares represent valid IVs identified by Guo et al. (2018)'s procedure. (c) Results from Guo et al. (2018) with pseudos included. The orange dot-dashed line separates pseudo and real genetic variants. Green triangles refer to SNPs identified as invalid. The blue squares are SNPs identified as valid instruments.

(Barber & Candes, 2019).

We close this section by performing additional numerical studies to explore the uncertainty of the aforementioned results, due to the randomness induced by generating pseudo variants. We run the procedure 50 times by repeatedly permuting the true SNP design matrix to generate pseudos. 47 out of 50 runs give negative effect estimates and the median of causal effect estimates from each run is -0.033 . For comparison, we also repeat TSHT with voting to the same candidate set used in our procedure 50 times. The median of resulting effect estimates is -0.010 and 50 out of 50 runs give negative effect estimates.

References

- ANGRIST, J. D. & KEUEGER, A. B. (1991). Does compulsory school attendance affect schooling and earnings? *The Quarterly Journal of Economics* **106**, 979–1014.
- BARBER, R. F. & CANDES, E. J. (2015). Controlling the false discovery rate via knockoffs. *Ann. Statist.* **43**, 2055–2085.
- BARBER, R. F. & CANDES, E. J. (2019). A knockoff filter for high-dimensional selective inference. *Ann. Statist.* **47**, 2504–2537.
- BOUND, J., JAEGER, D. A. & BAKER, R. M. (1995). Problems with instrumental variables estimation when the correlation between the instruments and the endogenous explanatory variable is weak. *J Am Statist Assoc.* **90**, 443–450.
- BOWDEN, J., SMITH, G. D. & BURGESS, S. (2015). Mendelian randomization with invalid instruments: effect estimation and bias detection through Egger regression. *Int. J. Epidemiol.* **44**, 512–525.
- BOWDEN, J., SMITH, G. D., HAYCOCK, P. C. & BURGESS, S. (2016). Consistent estimation in Mendelian randomization with some invalid instruments using a weighted median estimator. *Genet. Epidemiol.* **40**, 304–314.
- BROWNING, S. (2008). Missing data imputation and haplotype phase inference for genome-wide association studies. *Hum Genet.* **124**, 439–450.
- BURGESS, S., BOWDEN, J., DUDBRIDGE, F. & THOMPSON, S. G. (2016). Assessing the effectiveness of robust instrumental variable methods using multiple candidate instruments with application to Mendelian randomization. *Preprint arXiv:1606.03729*.
- BURGESS, S., TIMPSON, N. J., EBRAHIM, S. & SMITH, G. D. (2015). Mendelian randomization: where are we now and where are we going? *Int J Epidemiol.* **44**, 379–388.

- CARRASCO, M. (2012). A regularization approach to the many instruments problem. *J. Econom.* **170**, 383–398.
- CARRASCO, M. & TCHUENTE, G. (2015). Regularized LIML for many instruments. *J. Econom.* **186**, 427–442.
- DE BAKKER, P. I., FERREIRA, M. A., JIA, X., NEALE, B. M., RAYCHAUDHURI, S. & VOIGHT, B. F. (2008). Practical aspects of imputation-driven meta-analysis of genome-wide association studies. *Hum Mol Genet.* **17**, R122–R128.
- DIDELEZ, V. & SHEEHAN, N. (2007). Mendelian randomization as an instrumental variable approach to causal inference. *Stat Methods Med Res.* **16**, 309–330.
- DONALD, S. G. & NEWHEY, W. K. (2001). Choosing the number of instruments. *Econometrica.* **69**, 1161–1191.
- DONOHO, D. (1995). De-noising by soft-thresholding. *IEEE Trans. Inform. Theory* **41**, 613–627.
- DONOHO, D. L. & JOHNSTONE, I. M. (1994). Ideal spatial adaptation by wavelet shrinkage. *Biometrika.* **81**, 425–455.
- ECKLES, D., KIZILCEC, R. F. & BAKSHY, E. (2016). Estimating peer effects in networks with peer encouragement designs. *Proceedings of the National Academy of Sciences* **113**, 7316–7322.
- FAN, J. & LV, J. (2008). Sure independence screening for ultrahighdimensional feature space. *J. R. Statist. Soc. B.* **70**, 849–911.
- FONTAINE, K. R., CHESKIN, L. J. & BAROFSKY, I. (1996). Health-related quality of life in obese persons seeking treatment. *J Fam Pract.* **43**, 265–270.
- GOLDMAN, M. & RAO, J. (2016). Experiments as instruments: Heterogeneous position effects in sponsored search auctions. *EAI Endorsed Trans. Serious Games* **3**, e2.
- GUO, Z., KANG, H., CAI, T. T. & SMALL, D. S. (2018). Confidence intervals for causal effects with invalid instruments by using two-stage hard thresholding with voting. *J. R. Statist. Soc. B.* **80**, 793–815.
- HAN, C. (2008). Detecting invalid instruments using l_1 -gmm. *Econ. Lett.* **101**, 285–287.
- HARTFORD, J. S., VEITCH, V., SRIDHAR, D. & LEYTON-BROWN, K. (2021). Valid causal inference with (some) invalid instruments. *ICML.* **139**, 4096–4106.
- HERD, P., CARR, D. & ROAN, C. (2014). Cohort Profile: Wisconsin Longitudinal Study (WLS). *Int. J. Epidemiol.* **43**, 34–41.

- HOWIE, B., MARCHINI, J. & STEPHENS, M. (2011). Genotype imputation with thousands of genomes. *G3 (Bethesda)*. **1**, 457–470.
- HOWIE, B. N., DONNELLY, P. & MARCHINI, J. (2009). A flexible and accurate genotype imputation method for the next generation of genome-wide association studies. *PLoS Genet* **5**, e1000529.
- JAVANMARD, A. & MONTANARI, A. (2014). Confidence intervals and hypothesis testing for high-dimensional regression. *J. Mach. Learn. Res.* **15**, 2869–2909.
- KANG, H., ZHANG, A., CAI, T. T. & SMALL, D. S. (2016). Instrumental variables estimation with some invalid instruments and its application to Mendelian randomization. *J. Am. Statist. Ass.* **111**, 132–144.
- KATZ, D. A., MCHORNEY, C. A. & ATKINSON, R. L. (2000). Impact of obesity on health-related quality of life in patients with chronic illness. *J Gen Intern Med.* **15**, 789–796.
- KOLESAR, M., CHETTY, R., FRIEDMAN, J., GLAESER, E. & IMBENS, G. W. (2015). Identification and inference with many invalid instruments. *J. Bus. Econ. Statist.* **33**, 474–484.
- LAURIE, C. C., DOHENY, K. F., MIREL, D. B. et al. (2010). Quality control and quality assurance in genotypic data for genome-wide association studies. *Genet Epidemiol.* **34**, 591–602.
- LAWLOR, D. A., HARBORD, R. M., STERNE, J. A. C., TIMPSON, N. & SMITH, G. D. (2008). Mendelian randomization: Using genes as instruments for making causal inferences in epidemiology. *Statist. Med.* **27**, 1133–1163.
- LI, Y., WILLER, C., SANNA, S. & ABECASIS, G. (2009). Genotype imputation. *Annu Rev Genomics Hum Genet.* **10**, 387–406.
- LI, Y., WILLER, C. J., DING, J., SCHEET, P. & ABECASIS, G. R. (2010). MaCH: Using sequence and genotype data to estimate haplotypes and unobserved genotypes. *Genet Epidemiol.* **34**, 816–834.
- MARCHINI, J., HOWIE, B., MYERS, S., MCVEAN, G. & DONNELLY, P. (2007). A new multi-point method for genome-wide association studies by imputation of genotypes. *Nat. Genet.* **39**, 906–913.
- MORRISON, J., KNOBLAUCH, N., MARCUS, J. H. et al. (2020). Mendelian randomization accounting for correlated and uncorrelated pleiotropic effects using genome-wide summary statistics. *Nat. Genet.* **52**, 740–747.
- MYERS, A. & ROSEN, J. C. (1999). Obesity stigmatization and coping: relation to mental health symptoms, body image, and self-esteem. *Int J Obes Relat Metab Disord.* **23**, 221–230.

- NELSON, C. R. & STARTZ, R. (1990a). The distribution of the instrumental variables estimator and its t-ratio when the instrument is a poor one. *J Bus.* **63**, S125–S140.
- NELSON, C. R. & STARTZ, R. (1990b). Some further results on the exact small sample properties of the instrumental variable estimator. *Econometrica.* **58**, 967–976.
- PATTERSON, N., PRICE, A. L. & REICH, D. (2006). Population structure and eigenanalysis. *PLoS Genet.* **2**, e190.
- PEYSAKHOVICH, A. & ECKLES, D. (2018). Learning causal effects from many randomized experiments using regularized instrumental variables. In *Proceedings of the 2018 World Wide Web Conference*.
- SANDERSON, E., RICHARDSON, T. G., HEMANI, G. & SMITH, G. D. (2021). The use of negative control outcomes in Mendelian randomization to detect potential population stratification. *Int J Epidemiol.* **50**, 1350–1361.
- SCHEET, P. & STEPHENS, M. (2006). A fast and flexible statistical model for large-scale population genotype data: Applications to inferring missing genotypes and haplotypic phase. *Am. J. Hum. Genet.* **78**, 629–644.
- SMITH, G. D. (2007). Capitalizing on Mendelian randomization to assess the effects of treatments. *J R Soc Med.* **100**, 432–435.
- STOCK, J. H., WRIGHT, J. H. & YOGO, M. (2002). A survey of weak instruments and weak identification in generalized method of moments. *J Bus Econ Stat.* **20**, 518–529.
- STOCK, J. H. & YOGO, M. (2005). *Testing for Weak Instruments in Linear IV Regression*, chap. 5. Cambridge University Press, pp. 80–108.
- WANG, L. & TCHETGEN TCHETGEN, E. (2018). Bounded, efficient and multiply robust estimation of average treatment effects using instrumental variables. *J. R. Statist. Soc. B.* **80**, 531–550.
- WINDMEIJER, F., FARBMACHER, H., DAVIES, N. & SMITH, G. D. (2019). On the use of the lasso for instrumental variables estimation with some invalid instruments. *J. Am. Statist. Ass.* **114**, 1339–1350.
- WINDMEIJER, F. A., LIANG, X., HARTWIG, F. P. & BOWDEN, J. (2021). The confidence interval method for selecting valid instrumental variables. *J. R. Statist. Soc. B.* **83**, 752–776.
- WU, Y., BOOS, D. D. & STEFANSKI, L. A. (2007). Controlling variable selection by the addition of pseudovariables. *J. Am. Statist. Ass.* **102**, 235–243.

ZHAO, Q., WANG, J., HEMANI, G., BOWDEN, J. & SMALL, D. S. (2020). Statistical inference in two-sample summary-data Mendelian randomization using robust adjusted profile score. *Ann. Statist.* **48**, 1742–1769.

Supplementary Materials

The supplementary file is organized as follows. We introduce the sample splitting algorithm in Section S1. More details on our real data application are provided in Section S2. We introduce the notations in Section S3. Additional simulations to demonstrate the robustness of the proposed method are presented in Section S4.

S1 Alternative Algorithm by Sample Splitting

To deal with the effect of selection bias and perform statistical inference on the causal effect estimate, we consider the sample splitting version of the proposed method. Specifically, we split the sample into two halves: H_1 and H_2 . The sizes of H_1 and H_2 are denoted by n_1 and n_2 respectively, which satisfy $n_1 + n_2 = n$ and $n_1 = cn_2$ for some constant $c > 0$. In our numerical experiments, we take $c = 1.5$. Let $\mathbb{Z}^{(1)} \in \mathbb{R}^{n_1 \times p}$, $\mathbf{D}^{(1)} \in \mathbb{R}^{n_1}$ and $\mathbf{Y}^{(1)} \in \mathbb{R}^{n_1}$ denote the collection of data in H_1 , and correspondingly $\mathbb{Z}^{(2)} \in \mathbb{R}^{n_2 \times p}$, $\mathbf{D}^{(2)} \in \mathbb{R}^{n_2}$ and $\mathbf{Y}^{(2)} \in \mathbb{R}^{n_2}$ represent the data in H_2 . To find spurious instruments, we generate p pseudo variables on H_1 by randomly permuting the rows of $\mathbb{Z}^{(1)}$. Let $\mathbb{Z}^{(1)*}$ be the design matrix associated with pseudo variables. Combine the p -dimensional pseudo variables with the initial p -dimensional candidate instruments, and we use $\tilde{\mathbb{Z}}^{(1)} \in \mathbb{R}^{n \times 2p}$ to denote the resulting design matrix.

S1.1 Estimation of valid instruments

First we fit the reduced form models (2.3) and (2.4) on the first subsample H_1 with design matrix $\tilde{\mathbb{Z}}^{(1)}$, and estimate the parameters $\gamma, \Gamma \in \mathbb{R}^p$ based on de-biased lasso, denoted by $\hat{\gamma}^{(1)}$ and $\hat{\Gamma}^{(1)}$. We also calculate the standard error $\text{SE}(\hat{\gamma}_l^{(1)})$ for $1 \leq l \leq 2p$. We refer to (3.1) and (3.2) in the main paper for more details on the de-biased lasso estimators and their estimated standard errors. To further estimate the set of relevant instruments that are conditionally associated with the exposure, we implement the joint thresholding and let $\hat{\mathcal{S}}_1 = \{l : 1 \leq l \leq 2p, |\hat{\gamma}_l^{(1)}| \geq \delta_n \times \text{SE}(\hat{\gamma}_l^{(1)})\}$ denote the set of candidates passing the joint thresholding, where $\delta_n = \sqrt{\omega \log(\max\{n_1, 2p\})}$. Next, locate spurious instruments by estimating the range of causal effect estimates from pseudo variables in $\hat{\mathcal{S}}_1$ and remove them from the candidate set. The remaining set is represented by $\hat{\mathcal{S}}_2$ with cardinality q and let $\mathbf{Z}_{\hat{\mathcal{S}}_2} \in \mathbb{R}^q$ denote the associated candidate instruments.

Henceforth, we focus on the second subsample H_2 . Consider models (2.1) and (2.2) with \mathbf{Z} replaced by $\mathbf{Z}_{\hat{\mathcal{S}}_2}$, and parameters γ, π substituted by $\gamma_{\hat{\mathcal{S}}_2}, \pi_{\hat{\mathcal{S}}_2}$. And the true values are $\gamma_{\hat{\mathcal{S}}_2}^*, \pi_{\hat{\mathcal{S}}_2}^*$. We will account for the probability that this replacement fails at the end. Similarly, the reduced form parameter Γ would become $\Gamma_{\hat{\mathcal{S}}_2} = \pi_{\hat{\mathcal{S}}_2} + \beta\gamma_{\hat{\mathcal{S}}_2}$. We use $\mathbb{Z}_{\hat{\mathcal{S}}_2}^{(2)} \in \mathbb{R}^{n_2 \times q}$ to denote the design matrix associated with $\hat{\mathcal{S}}_2$ on H_2 . Fit linear models for $\mathbf{D}^{(2)}, \mathbb{Z}_{\hat{\mathcal{S}}_2}^{(2)}$ and $\mathbf{Y}^{(2)}, \mathbb{Z}_{\hat{\mathcal{S}}_2}^{(2)}$ respectively. As

q is much smaller than n_2 , we apply OLS to obtain estimates $\hat{\gamma}_{\hat{\mathcal{S}}_2}^{(2)}, \hat{\Gamma}_{\hat{\mathcal{S}}_2}^{(2)} \in \mathbb{R}^q$, and calculate the standard error of $\hat{\gamma}_{\hat{\mathcal{S}}_2, l}^{(2)}$ for $1 \leq l \leq q$,

$$\text{SE}(\hat{\gamma}_{\hat{\mathcal{S}}_2, l}^{(2)}) = \sqrt{\frac{\left[\left(\mathbb{Z}_{\hat{\mathcal{S}}_2}^{(2)\top} \mathbb{Z}_{\hat{\mathcal{S}}_2}^{(2)} \right)^{-1} \right]_{ll} \|\mathbf{D}^{(2)} - \mathbb{Z}_{\hat{\mathcal{S}}_2}^{(2)} \hat{\gamma}_{\hat{\mathcal{S}}_2}^{(2)}\|_2^2}{n_2}}.$$

Then we apply another joint thresholding by comparing $|\hat{\gamma}_{\hat{\mathcal{S}}_2, l}^{(2)}|$ with $\delta_n \times \text{SE}(\hat{\gamma}_{\hat{\mathcal{S}}_2, l}^{(2)})$. Here $\delta_n = \sqrt{\omega \log n_2}$. Let $\tilde{\mathcal{S}}_2 \subset \{1, \dots, q\}$ be the index set of candidates passing this joint thresholding on the second portion of data.

For $j \in \tilde{\mathcal{S}}_2$, calculate causal estimate $\hat{\beta}^{(2, j)} = \hat{\Gamma}_{\hat{\mathcal{S}}_2, j}^{(2)} / \hat{\gamma}_{\hat{\mathcal{S}}_2, j}^{(2)}$, where $\hat{\beta}^{(2, j)}$ represents the j th estimate obtained from the subsample H_2 .

Take $\hat{\beta}^{(2, j)}$ as the underlying truth and compute the bias for estimate $\hat{\beta}^{(2, l)}$ for $l \in \tilde{\mathcal{S}}_2$, denoted by $\hat{b}^{(2, j, l)} = \hat{\beta}^{(2, l)} - \hat{\beta}^{(2, j)}$, and the standard error $\text{SE}(\hat{b}^{(2, j, l)})$. We discuss details of $\text{SE}(\hat{b}^{(2, j, l)})$ in the supplementary materials. The candidate l votes for j if their causal estimates are similar, and numerically $|\hat{b}^{(2, j, l)}|$ below a threshold, that is, $|\hat{b}^{(2, j, l)}| \leq \text{SE}(\hat{b}^{(2, j, l)}) \sqrt{\omega^2 \log n_2}$. Here we use ω^2 instead ω since we are conducting pairwise tests. Note that $\hat{b}^{(2, j, l)}$ remains the same if we swap j, l , which implies that if $|\hat{b}^{(2, j, l)}|$ pass the threshold, then the candidate j would be also in favor of l by symmetry. Summing up $\mathbb{1}(|\hat{b}^{(2, j, l)}| \leq \text{SE}(\hat{b}^{(2, j, l)}) \sqrt{\omega^2 \log n_2})$ over $l \in \tilde{\mathcal{S}}_2$ gives the total votes that candidate j gets, denoted by V_j , which also equals V_l by symmetry. For the collection of $j \in \tilde{\mathcal{S}}_2$ such that j gets the most votes, we estimate it as the set of valid instruments, denoted by $\hat{\mathcal{S}}_3$.

S1.2 Estimation of causal effect and statistical inference

We borrow the idea from [Guo et al. \(2018\)](#) for the construction of causal effect estimate and its associated confidence interval. On the second subsample H_2 , we estimate the causal effect as follows

$$\hat{\beta}_{\text{split}} = \frac{\{\hat{\gamma}_{\hat{\mathcal{S}}_2, \hat{\mathcal{S}}_3}^{(2)}\}^\top \widehat{\mathbf{W}} \hat{\Gamma}_{\hat{\mathcal{S}}_2, \hat{\mathcal{S}}_3}^{(2)}}{\{\hat{\gamma}_{\hat{\mathcal{S}}_2, \hat{\mathcal{S}}_3}^{(2)}\}^\top \widehat{\mathbf{W}} \hat{\gamma}_{\hat{\mathcal{S}}_2, \hat{\mathcal{S}}_3}^{(2)}}, \quad (\text{S1.1})$$

where $\hat{\gamma}_{\hat{\mathcal{S}}_2, \hat{\mathcal{S}}_3}^{(2)}$ is subvector of $\hat{\gamma}_{\hat{\mathcal{S}}_2}^{(2)}$ indexed by $\hat{\mathcal{S}}_3$ and similarly for $\hat{\Gamma}_{\hat{\mathcal{S}}_2, \hat{\mathcal{S}}_3}^{(2)}$. The weighting matrix

$$\widehat{\mathbf{W}} = [\hat{\Sigma}_{\hat{\mathcal{S}}_2}^{(2)}]_{\hat{\mathcal{S}}_3, \hat{\mathcal{S}}_3} - [\hat{\Sigma}_{\hat{\mathcal{S}}_2}^{(2)}]_{\hat{\mathcal{S}}_3, \hat{\mathcal{S}}_3^c} \left\{ [\hat{\Sigma}_{\hat{\mathcal{S}}_2}^{(2)}]_{\hat{\mathcal{S}}_3^c, \hat{\mathcal{S}}_3^c} \right\}^{-1} [\hat{\Sigma}_{\hat{\mathcal{S}}_2}^{(2)}]_{\hat{\mathcal{S}}_3^c, \hat{\mathcal{S}}_3} \quad (\text{S1.2})$$

with $\hat{\Sigma}_{\hat{\mathcal{S}}_2}^{(2)}$ representing the sample covariance matrix of candidate instruments corresponding to $\hat{\mathcal{S}}_2$ on the second subsample H_2 , i.e., $\hat{\Sigma}_{\hat{\mathcal{S}}_2}^{(2)} = \{\mathbb{Z}_{\hat{\mathcal{S}}_2}^{(2)}\}^\top \mathbb{Z}_{\hat{\mathcal{S}}_2}^{(2)} / n_2$, and $[\hat{\Sigma}_{\hat{\mathcal{S}}_2}^{(2)}]_{\mathcal{I}_1, \mathcal{I}_2}$ is formed by rows and columns of $\hat{\Sigma}_{\hat{\mathcal{S}}_2}^{(2)}$ indexed by \mathcal{I}_1 and \mathcal{I}_2 respectively.

The asymptotic variance of $\hat{\beta}_{\text{split}}$ is given by $(\alpha_Y^{*2}\sigma_u^2 + \sigma_Y^2)/v_{\text{split}}$ with

$$v_{\text{split}} = \gamma_{\hat{\mathcal{S}}_2, \mathcal{T}_*}^{*\text{T}} \left([\Sigma_{\hat{\mathcal{S}}_2}]_{\mathcal{T}_*, \mathcal{T}_*} - [\Sigma_{\hat{\mathcal{S}}_2}]_{\mathcal{T}_*, \mathcal{T}_*^c} \left\{ [\Sigma_{\hat{\mathcal{S}}_2}]_{\mathcal{T}_*^c, \mathcal{T}_*^c} \right\}^{-1} [\Sigma_{\hat{\mathcal{S}}_2}]_{\mathcal{T}_*^c, \mathcal{T}_*} \right) \gamma_{\hat{\mathcal{S}}_2, \mathcal{T}_*}^*, \quad (\text{S1.3})$$

and it is estimated by

$$\hat{v}_{\text{split}} = \widehat{\text{var}}(\hat{\beta}_{\text{split}}) = \frac{\hat{\Theta}_{11} + \hat{\beta}_{\text{split}}^2 \hat{\Theta}_{22} - 2\hat{\beta}_{\text{split}} \hat{\Theta}_{12}}{\{\hat{\gamma}_{\hat{\mathcal{S}}_2, \hat{\mathcal{S}}_3}^{(2)}\}^{\text{T}} \widehat{\mathbf{W}} \hat{\gamma}_{\hat{\mathcal{S}}_2, \hat{\mathcal{S}}_3}^{(2)}}, \quad (\text{S1.4})$$

where

$$\begin{aligned} \hat{\Theta}_{11} &= \frac{1}{n_2} \left\| \mathbf{Y}^{(2)} - \mathbb{Z}_{\hat{\mathcal{S}}_2}^{(2)} \hat{\Gamma}_{\hat{\mathcal{S}}_2}^{(2)} \right\|_2^2, \\ \hat{\Theta}_{22} &= \frac{1}{n_2} \left\| \mathbf{D}^{(2)} - \mathbb{Z}_{\hat{\mathcal{S}}_2}^{(2)} \hat{\gamma}_{\hat{\mathcal{S}}_2}^{(2)} \right\|_2^2, \\ \hat{\Theta}_{12} &= \frac{1}{n_2} \left(\mathbf{Y}^{(2)} - \mathbb{Z}_{\hat{\mathcal{S}}_2}^{(2)} \hat{\Gamma}_{\hat{\mathcal{S}}_2}^{(2)} \right)^{\text{T}} \left(\mathbf{D}^{(2)} - \mathbb{Z}_{\hat{\mathcal{S}}_2}^{(2)} \hat{\gamma}_{\hat{\mathcal{S}}_2}^{(2)} \right). \end{aligned} \quad (\text{S1.5})$$

We then can further obtain the $100(1 - \alpha)\%$ confidence interval for β :

$$\left[\hat{\beta}_{\text{split}} - z_{1-\alpha/2} \sqrt{\hat{v}_{\text{split}}/n_2}, \hat{\beta}_{\text{split}} + z_{1-\alpha/2} \sqrt{\hat{v}_{\text{split}}/n_2} \right], \quad (\text{S1.6})$$

where $z_{1-\alpha/2}$ is the $(1 - \alpha/2)$ -quantile of the standard normal distribution. The procedure with sample splitting is summarized in Algorithm [S1](#).

S2 More Details on Data Application

S2.1 Acknowledgments

Our analysis uses data from the Wisconsin Longitudinal Study (WLS). The WLS genetic data is sponsored by the National Institute on Aging (grant numbers R01AG009775, R01AG033285, and R01AG041868) and was conducted by the University of Wisconsin. More information can be found at <https://www.ssc.wisc.edu/wlsresearch/>.

S2.2 Relationship between BMI and HUI-3

We display the observed relationship between BMI and Health Utility Index Mark 3 (HUI-3) in Figure [S1](#). We can learn from Figure [S1](#)-(a) that HUI-3 has a positive association with BMI when BMI is lower than 25, and is negatively associated with BMI when BMI is higher than 25. This is consistent with the fact that both underweight and overweight are linked with a range of adverse

Algorithm S1 Fighting noise with noise – sample splitting

INPUT: Design matrix $\mathbb{Z} \in \mathbb{R}^{n \times p}$, observed exposure $\mathbf{D} \in \mathbb{R}^n$, observed outcome $\mathbf{Y} \in \mathbb{R}^n$.

00. Divide data into two halves:

H_1 of size n_1 and H_2 of size n_2 ;

Denote the associated data as $\mathbb{Z}^{(1)} \in \mathbb{R}^{n_1 \times p}$, $\mathbf{D}^{(1)} \in \mathbb{R}^{n_1}$, $\mathbf{Y}^{(1)} \in \mathbb{R}^{n_1}$, and $\mathbb{Z}^{(2)} \in \mathbb{R}^{n_2 \times p}$, $\mathbf{D}^{(2)} \in \mathbb{R}^{n_2}$, $\mathbf{Y}^{(2)} \in \mathbb{R}^{n_2}$.

0. Pseudo variables generation on H_1 :

Generate p pseudo variables $Z_{p+1}^{(1)}, \dots, Z_{2p}^{(1)}$ by randomly permuting the rows of $\mathbb{Z}^{(1)}$;

Denote the resulting design matrix as $\mathbb{Z}^{(1)*}$, and the concatenation of \mathbb{Z} and $\mathbb{Z}^{(1)*}$ as $\tilde{\mathbb{Z}}^{(1)}$.

1. Joint thresholding on H_1 :

Fit a linear model for $\mathbf{D}^{(1)} \sim \tilde{\mathbb{Z}}^{(1)}$: let $\hat{\gamma}^{(1)}$ be the debiased lasso estimate (Javanmard & Montanari, 2014). Also obtain their standard error estimate $\text{SE}(\hat{\gamma}_l^{(1)})$.

Fit a linear model for $\mathbf{Y}^{(1)} \sim \tilde{\mathbb{Z}}^{(1)}$ and obtain the estimate $\hat{\Gamma}^{(1)}$ in a similar fashion.

Estimate the relevant variables $\hat{\mathcal{S}}_1 = \{l \in [2p] : |\hat{\gamma}_l^{(1)}| \geq \delta_n \times \text{SE}(\hat{\gamma}_l^{(1)})\}$, where $\delta_n = \sqrt{\omega \log(\max\{n_1, 2p\})}$, where ω is a tuning parameter. Denote pseudos in $\hat{\mathcal{S}}_1$ by $\hat{\mathcal{P}}$.

2. Irrelevant variables removal:

For $l \in \hat{\mathcal{S}}_1$, calculate causal effect estimate $\hat{\beta}^{(1,l)} = \hat{\Gamma}_l^1 / \hat{\gamma}_l^{(1)}$;

Remove variables similar to pseudo variables in their causal effect estimate $\hat{\beta}^{(1,l)}$ from $\hat{\mathcal{S}}_1$:

$$\hat{\mathcal{S}}_2 = \hat{\mathcal{S}}_1 \setminus \left\{ l \in \hat{\mathcal{S}}_1 : \min_{j \in \hat{\mathcal{P}}} \hat{\beta}^{(1,j)} \leq \hat{\beta}^{(1,l)} \leq \max_{j \in \hat{\mathcal{P}}} \hat{\beta}^{(1,j)} \right\}.$$

Denote the cardinality of $\hat{\mathcal{S}}_2$ as q .

Algorithm S1 (continue)

3. Joint thresholding on H_2 :

Let $\mathbb{Z}_{\hat{\mathcal{S}}_2}^{(2)} \in \mathbb{R}^{n_2 \times q}$ denote the associated design matrix of $\hat{\mathcal{S}}_2$ on H_2 . Fit a linear model for $\mathbf{D}^{(2)} \sim \mathbb{Z}_{\hat{\mathcal{S}}_2}^{(2)}$: obtain the OLS estimator $\hat{\gamma}_{\hat{\mathcal{S}}_2}^{(2)}$ and standard error estimate $\text{SE}(\hat{\gamma}_{\hat{\mathcal{S}}_2, l}^{(2)})$ for $1 \leq l \leq q$;

Fit a linear model for $\mathbf{Y}^{(2)} \sim \mathbb{Z}_{\hat{\mathcal{S}}_2}^{(2)}$ and obtain the estimate $\hat{\Gamma}_{\hat{\mathcal{S}}_2}^{(2)}$ in a similar fashion;

Further approximate the set of relevant instruments as $\tilde{\mathcal{S}}_2 = \{l \in [q] : |\hat{\gamma}_{\hat{\mathcal{S}}_2, l}^{(2)}| \geq \delta_n \times \text{SE}(\hat{\gamma}_{\hat{\mathcal{S}}_2, l}^{(2)})\}$, where $\delta_n = \sqrt{\omega \log n_2}$.

4. Symmetric voting on H_2 :

For $l \in \tilde{\mathcal{S}}_2$, calculate causal effect estimate $\hat{\beta}^{(2, l)} = \hat{\Gamma}_{\hat{\mathcal{S}}_2, l}^{(2)} / \hat{\gamma}_{\hat{\mathcal{S}}_2, l}^{(2)}$;

For $j, l \in \tilde{\mathcal{S}}_2$, compute $\hat{b}^{(2, j, l)} = \hat{\beta}^{(2, l)} - \hat{\beta}^{(2, j)}$ and $\text{SE}(\hat{b}^{(2, j, l)})$;

For $j \in \tilde{\mathcal{S}}_2$, find the number of candidates leading to a similar causal effect estimate with j :

$$V_j = \left| \left\{ l \in \tilde{\mathcal{S}}_2 : |\hat{b}^{(2, j, l)}| / \text{SE}(\hat{b}^{(2, j, l)}) \leq \sqrt{\omega^2 \log n_2} \right\} \right|;$$

Find valid IVs using the plurality rule:

$$\hat{\mathcal{S}}_3 = \left\{ j : V_j = \max_{l \in \tilde{\mathcal{S}}_2} V_l \right\}.$$

5. Causal effect estimation:

$$\hat{\beta}_{\text{split}} = \frac{\{\hat{\gamma}_{\hat{\mathcal{S}}_2, \hat{\mathcal{S}}_3}^{(2)}\}^T \widehat{\mathbf{W}} \hat{\Gamma}_{\hat{\mathcal{S}}_2, \hat{\mathcal{S}}_3}^{(2)}}{\{\hat{\gamma}_{\hat{\mathcal{S}}_2, \hat{\mathcal{S}}_3}^{(2)}\}^T \widehat{\mathbf{W}} \hat{\gamma}_{\hat{\mathcal{S}}_2, \hat{\mathcal{S}}_3}^{(2)}},$$

where $\hat{\gamma}_{\hat{\mathcal{S}}_2, \hat{\mathcal{S}}_3}^{(2)}$ is subvector of $\hat{\gamma}_{\hat{\mathcal{S}}_2}^{(2)}$ indexed by $\hat{\mathcal{S}}_3$ and similarly for $\hat{\Gamma}_{\hat{\mathcal{S}}_2, \hat{\mathcal{S}}_3}^{(2)}$. See (S1.2) for the explicit form of the weighting matrix $\widehat{\mathbf{W}}$.

Estimated variance of $\hat{\beta}_{\text{split}}$:

$$\hat{v}_{\text{split}} = \widehat{\text{var}}(\hat{\beta}_{\text{split}}) = \frac{\hat{\Theta}_{11} + \hat{\beta}_{\text{split}}^2 \hat{\Theta}_{22} - 2\hat{\beta}_{\text{split}} \hat{\Theta}_{12}}{\{\hat{\gamma}_{\hat{\mathcal{S}}_2, \hat{\mathcal{S}}_3}^{(2)}\}^T \widehat{\mathbf{W}} \hat{\gamma}_{\hat{\mathcal{S}}_2, \hat{\mathcal{S}}_3}^{(2)}},$$

where $\hat{\Theta}_{11}, \hat{\Theta}_{22}, \hat{\Theta}_{12}$ are given in (S1.5).

6. $100(1 - \alpha)\%$ confidence interval: $[\hat{\beta}_{\text{split}} - z_{1-\alpha/2} \sqrt{\hat{v}_{\text{split}}/n_2}, \hat{\beta}_{\text{split}} + z_{1-\alpha/2} \sqrt{\hat{v}_{\text{split}}/n_2}]$.

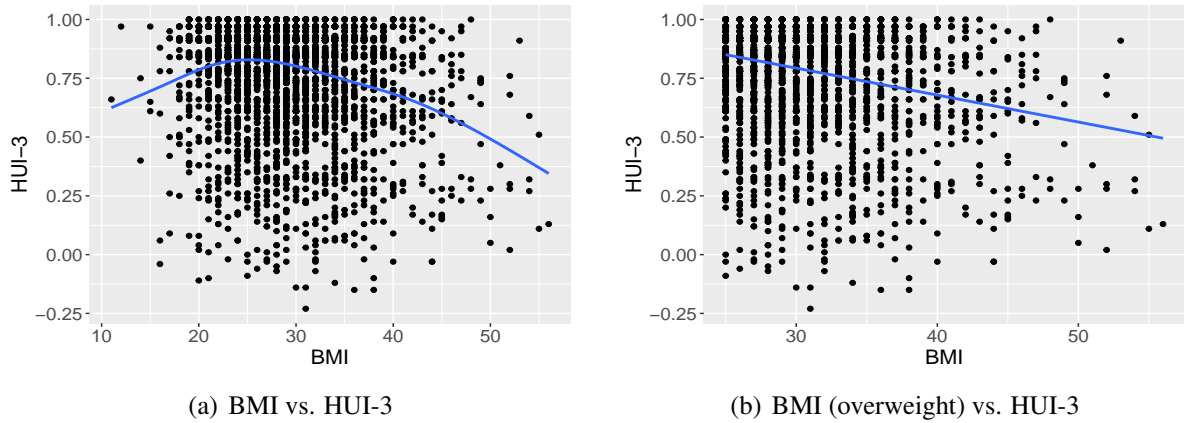


Figure S1: The plot on the left panel depicts the relationship between BMI and Health Utility Index Mark 3 (HUI-3) for the WLS data used in our analysis. On the right panel, we zoom in on BMI above 25 and HUI-3 accordingly.

health conditions. Meanwhile, the healthy weight range is between 18.5 and 24.9. We provide additional plot in Figure S1-(b) to emphasize that as BMI increases over 25, the risk for lower quality of life increases, which is our focus in the data application.

S2.3 WLS Data Pre-processing

For genomic data, we use imputed genetic variants extracted from whole-genome sequencing on 22 chromosomes, in which unobserved genotypes in the study sample are estimated from the haplotype or genotype reference panel (Browning, 2008; Li et al., 2009). This allows us to examine the evidence for association at biomarkers that are not directly genotyped (Scheet & Stephens, 2006; Marchini et al., 2007; Browning, 2008). The input of missing data imputation are observed variants that meet criterion of quality control: for example, missing call rate $< 2\%$, minor allele frequency (MAF) ≥ 0.01 , Hardy-Weinberg Equilibrium (HWE) p -value $\geq 10^{-4}$, with known and unique positions, etc. See the genotype quality control report attached to Herd et al. (2014), which follows the quality filters described in Laurie et al. (2010). Genotype imputation were performed using IMPUTE2 software (Howie et al., 2009, 2011). To account for uncertainty of the imputation output, we exclude variants with BEAGLE allelic r^2 less than 0.3, which is an assessment of genotype imputation performance (de Bakker et al., 2008; Li et al., 2010).

For the remaining missing values in genotype data after matching with available phenotypes, we replace them by random sampling from the empirical allele distribution. Namely, the missing values at a genetic variant j are sampled from the associated marginal allele empirical distribution. In addition, there might be identical columns in our current SNP matrix, in which rows are indexed by graduates considered in our analysis and columns are indexed by genotypes. To proceed, we keep unique ones in our analysis and recheck at the end whether any excluded variants have exactly

the same (0,1,2) genotype representation as our estimated valid IVs. If there are any, they will also be identified as valid instruments.

S3 Notations

For any vector $\mathbf{v} \in \mathbb{R}^p$, v_j represents the j th element of \mathbf{v} . $\|\mathbf{v}\|_1$, $\|\mathbf{v}\|_2$ and $\|\mathbf{v}\|_\infty$ represent the usual 1-, 2- and ∞ - norms respectively. For a set S , $|S|$ denotes its cardinality and S^c is the complement of S . If $S \subset \{1, \dots, p\}$ is an index set, then $\mathbf{v}_S \in \mathbb{R}^{|S|}$ is a subvector of $\mathbf{v} \in \mathbb{R}^p$ indexed by S and $v_{S,l}$ denotes the l th element of \mathbf{v}_S for $1 \leq l \leq |S|$. For an $n \times p$ matrix $\mathbf{A} \in \mathbb{R}^{n \times p}$, we denote the (i, j) th element of \mathbf{A} by A_{ij} , the i th row as \mathbf{A}_i and the j th column as $\mathbf{A}_{.j}$. \mathbf{A}^T denotes the transpose of \mathbf{A} . $\|\mathbf{A}\|_\infty = \max_{1 \leq i, j \leq p} |A_{ij}|$ represents the maximum of the absolute element of matrix \mathbf{A} and $\|\mathbf{A}\|_1 = \max_{1 \leq j \leq n} \sum_{i=1}^p |A_{ij}|$ is the maximum absolute column sum of \mathbf{A} . For a symmetric matrix \mathbf{A} , let $\lambda_{\min}(\mathbf{A})$ and $\lambda_{\max}(\mathbf{A})$ denote the smallest and the largest eigenvalues respectively. The spectral norm $\|\mathbf{A}\|_2 = \lambda_{\max}(\mathbf{A})$. For functions $f(n)$ and $g(n)$, we write $f(n) = O(g(n))$ if $\lim_{n \rightarrow \infty} f(n)/g(n) = c$, where c is some constant. Particularly, if $g(n) = c$, the notation becomes $f(n) = O(1)$. Similarly, if $\lim_{n \rightarrow \infty} f(n)/g(n) = 0$, we write $f(n) = o(g(n))$. Specifically, if $g(n) = c$, we write $f(n) = o(1)$. The notation $a_n \lesssim c_n$ represents that there exists a constant C such that $a_n \leq Cb_n$ and $a_n \gtrsim b_n$ means that there exists a constant c such that $a_n \geq cb_n$. And $a_n \asymp d_n$ represents $a_n = \tilde{c}b_n$ for some constant \tilde{c} . $\text{cor}(X, Y)$ represents correlation between random variables X and Y , and let $\text{cov}(X, Y)$ denote the associated covariance. If $\mathbf{X} \in \mathbb{R}^p$ and $\mathbf{Y} \in \mathbb{R}^q$ are random vectors, then $\text{cov}(\mathbf{X}, \mathbf{Y}) \in \mathbb{R}^{p \times q}$ is the cross-covariance matrix.

S4 Additional Simulations

To further examine the performance and show the robustness of the proposed procedure, we consider additional settings and other competing methods in numerical experiments. To show the superior performance of the newly proposed mode-finding procedure compared to the voting procedure proposed in Guo et al. (2018), in addition to our proposed method in Algorithm 1, TSHT with voting (Guo et al., 2018) and sample splitting in Algorithm S1, we also compare with the approach that replaces the mode-finding step in our procedure with the voting proposed in Guo et al. (2018) but keeps all the other steps of our method. We call this method ‘‘Proposed (Voting-TSHT)’’. Simulation results of ‘‘Proposed (Voting-TSHT)’’ under the simulation setting in the main paper are displayed in section S4.1. Finite sample performances of the proposed method in comparison with several other approaches in the presence of weak instruments are collected in section S4.2. In section S4.3, we carry out numerical studies, in which the ‘‘independence’’ IV assumption is violated, that is, invalid instrument can be correlated with the unobserved confounding U . Additionally, we consider the setting where some irrelevant variables are allowed to be correlated with valid instruments in section S4.4. A typical example of this scenario would be the linkage disequi-

librium in genetic studies. Furthermore, we compare our proposed method with other competing methods in the econometric literature that deal with weak instruments in section [S4.5](#).

S4.1 Comparison with other methods-simulation in main paper

Under the simulation setting in the main paper, we also compare with the proposed procedure with voting ([Guo et al., 2018](#)), denoted by “Proposed (Voting-TSHT)”. For completeness, we also reproduce the results from the proposed method shown in the main paper. The performance summaries are presented in Tables [S1](#) and [S2](#).

Table S1: Performance summary for “Proposed (Voting-TSHT)” under the setting in main paper across 1000 Monte Carlo runs with $n = 500$, $p = 50,000$ and various σ_D^2 . We make the numbers bold for the method with the best performance except for the oracle estimate. Standard errors are presented in the bracket if applicable

	Method	Bias $\times 10$ (SE $\times 10$)	RMSE $\times 10$	Coverage (Nominal = 95%)
$\sigma_D^2 = 0$	Proposed (Voting-TSHT)	-0.34(0.03)	0.92	0.91
	Proposed	-0.13(0.02)	0.55	0.92
$\sigma_D^2 = 4$	Proposed (Voting-TSHT)	-0.24(0.03)	0.90	0.90
	Proposed	-0.12(0.02)	0.71	0.92
$\sigma_D^2 = 8$	Proposed (Voting-TSHT)	-0.16(0.02)	0.66	0.92
	Proposed	-0.08(0.02)	0.57	0.93

In terms of bias, efficiency and validity of inference, one can see that the proposed method with the voting procedure in [Guo et al. \(2018\)](#) can also give satisfactory results, but the newly proposed mode-finding algorithm achieves better performance.

Table S2: Average number of invalid, valid IVs and irrelevant variables in \hat{S}_1 , \hat{S}_2 and \hat{S}_3 respectively under the setting in main paper across 1000 Monte Carlo runs. The results are based on $n = 500$ and $p = 50,000$

	Method	\hat{S}_1			\hat{S}_2			\hat{S}_3		
		Invalid	Valid	Irrelevant	Invalid	Valid	Irrelevant	Invalid	Valid	Irrelevant
$\sigma_D^2 = 0$	Proposed (Voting-TSHT)	2.00	5.00	17.34	2.00	5.00	2.05	0.00	3.22	1.04
	Proposed	2.00	5.00	17.34	2.00	5.00	2.05	0.00	4.30	0.58
$\sigma_D^2 = 4$	Proposed (Voting-TSHT)	2.00	5.00	20.10	2.00	4.98	2.03	0.00	3.44	1.09
	Proposed	2.00	5.00	20.10	2.00	4.98	2.03	0.00	4.18	0.58
$\sigma_D^2 = 8$	Proposed (Voting-TSHT)	1.99	4.99	22.76	1.99	4.95	1.95	0.00	3.76	1.18
	Proposed	1.99	4.99	22.76	1.99	4.95	1.95	0.00	4.31	0.80

Table [S2](#) indicates that although “Proposed (Voting-TSHT)” performs well in terms of bias, MSE and empirical coverage, compared to our mode-finding algorithm, the voting ([Guo et al.](#),

2018) step votes against more valid instruments and estimate them as invalid, and also misidentifies more spurious instruments as valid.

S4.2 Weak instruments-simulation 2

In this simulation, we consider a more general setting in which there are 7 strong valid instruments, 50 weak valid instruments and 2 invalid IVs. Candidate instruments Z_j , the unobserved confounding U and random error ϵ_Y are generated from independent standard normal distributions for $1 \leq j \leq p$. The random error ϵ_D follows $N(0, \sigma_D^2)$ with $\sigma_D^2 = 0, 4, 8$.

For the weak IVs, true parameter values of the relevance strength to the exposure in absolute value are randomly generated from uniform distribution on the interval $[0.01, 0.3]$. The absolute relevance strength of strong IVs are randomly generated from the the uniform distribution on the interval $[2.5, 3.5]$. To be more specific, other than parameters associated with weak IVs, true values of the other parameters are given by

$$\begin{aligned}\gamma_{1:9}^* &= (3.21, -2.78, 3.02, 3.16, 3.30, 3.10, -3.16, 2.72, -3.03)^T \\ \pi_{1:2}^* &= (-3.5, 3.5, 0, 0, \dots, 0)^T \\ \psi^* &= \phi^* = \mathbf{0} \\ \alpha_D^* &= 4; \alpha_Y^* = -3.\end{aligned}$$

Here $\gamma_{1:7}^*$ denotes the first nine elements in γ^* and analogously $\pi_{1:2}^*$ represents the first two components in π^* . The dimension of candidate instruments $p = 100,000$. Our comparison includes the proposed method (Proposed), sample splitting (Sample Splitting), two-stage hard thresholding with voting (TSHT) in Guo et al. (2018), the proposed procedure with the voting in Guo et al. (2018) (Proposed (Voting-TSHT)), and the oracle method by assuming that we know the valid instruments a priori. Simulation results are presented in Tables S3 and S4. In the tables, we use “Oracle (All IVs)” and “Oracle (Strong IVs)” to denote the oracle estimate calculated using all valid instruments (strong and weak) and the oracle estimate obtained using strong valid instruments only. Additionally, histograms of causal effect estimates under $\sigma_D^2 = 0$ are presented in Figure S2.

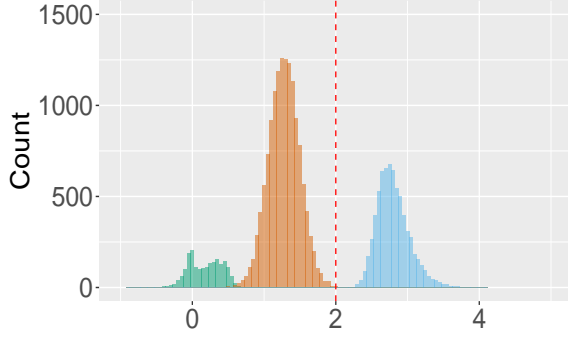
The proposed method performs well in the presence of weak instruments. The sample splitting gives slightly better performance in terms of bias and MSE when σ_D^2 is small, but it seems to overestimate the coverage probability under this setting. The TSHT with voting fails as it misidentifies spurious instruments as valid instruments. By comparing the results regarding “Oracle(All IVs)” and “Oracle(Strong IVs)”, one can find that weak instruments can introduce bias in causal effect estimate, which is consistent with existing literature (Nelson & Startz, 1990a; Stock & Yogo, 2005; Burgess et al., 2015).

Table S3: Performance summary for various methods and σ_D^2 under simulation 2 across 1000 Monte Carlo runs with $n = 500$ and $p = 100,000$. We make the numbers bold for the method with the best performance except the oracle estimate. Standard errors are presented in the bracket if applicable. For $SE < 0.005$, we report as $SE = 0.00$

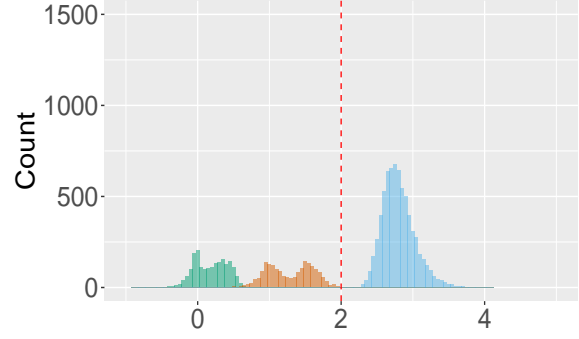
	Method	Bias $\times 10$ (SE $\times 10$)	RMSE $\times 10$	Coverage (Nominal = 95%)
$\sigma_D^2 = 0$	Proposed	-0.14(0.02)	0.70	0.92
	Sample Splitting	- 0.08(0.02)	0.58	0.99
	TSHT	-3.29(0.05)	3.62	0.01
	Proposed (Voting-TSHT)	-0.48(0.04)	1.23	0.82
	Oracle(All IVs)	-0.51(0.01)	0.58	0.59
	Oracle(Strong IVs)	-0.05(0.01)	0.32	0.95
$\sigma_D^2 = 4$	Proposed	-0.16(0.02)	0.76	0.91
	Sample Splitting	- 0.15(0.03)	0.94	0.98
	TSHT	-1.63(0.03)	1.81	0.05
	Proposed (Voting-TSHT)	-0.33(0.03)	0.97	0.84
	Oracle(All IVs)	-0.51(0.01)	0.58	0.59
	Oracle(Strong IVs)	-0.05(0.01)	0.32	0.95
$\sigma_D^2 = 8$	Proposed	- 0.16(0.02)	0.73	0.91
	Sample Splitting	-0.42(0.05)	1.75	0.95
	TSHT	-1.31(0.02)	1.44	0.08
	Proposed (Voting-TSHT)	-0.27(0.03)	0.84	0.87
	Oracle(All IVs)	-0.51(0.01)	0.58	0.58
	Oracle(Strong IVs)	-0.05(0.01)	0.32	0.95

Table S4: Average number of invalid, valid IVs and irrelevant variables in \hat{S}_1 , \hat{S}_2 and \hat{S}_3 under simulation 2 respectively across 1000 Monte Carlo runs. The results are based on $n = 500$ and $p = 100,000$. “-” stands for “inapplicable”

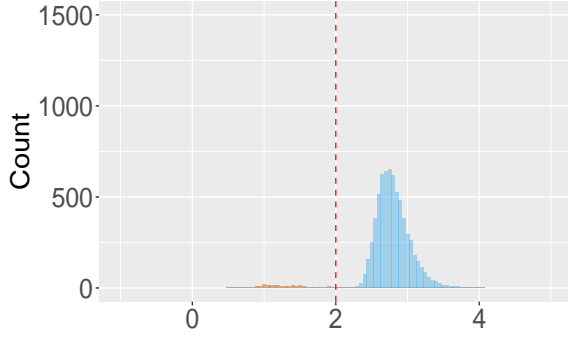
	Method	\hat{S}_1			\hat{S}_2			\hat{S}_3		
		Invalid	Valid	Irrelevant	Invalid	Valid	Irrelevant	Invalid	Valid	Irrelevant
$\sigma_D^2 = 0$	Proposed	2.00	7.01	13.97	2.00	7.00	2.00	0.00	6.62	0.19
	Sample Splitting	1.97	6.93	19.77	1.87	6.89	1.81	0.01	6.86	0.00
	TSHT	2.00	7.03	16.31	-	-	-	0.60	2.73	16.31
	Proposed (Voting-TSHT)	2.00	7.01	13.97	2.00	7.00	2.00	0.00	5.95	0.95
	Mode-Finding	2.00	7.03	16.31	-	-	-	0.73	3.47	16.24
$\sigma_D^2 = 4$	Proposed	2.00	7.01	17.67	2.00	6.99	1.97	0.00	6.62	0.49
	Sample Splitting	1.94	6.88	24.54	1.90	6.67	1.91	0.02	6.60	0.01
	TSHT	2.00	7.03	17.00	-	-	-	0.41	6.19	17.00
	Proposed (Voting-TSHT)	2.00	7.01	17.67	2.00	6.99	1.97	0.00	6.18	1.15
	Mode-Finding	2.00	7.03	17.00	-	-	-	0.58	6.58	16.99
$\sigma_D^2 = 8$	Proposed	2.00	7.01	20.72	2.00	6.91	1.97	0.01	6.67	0.79
	Sample Splitting	1.92	6.79	28.84	1.90	6.12	1.95	0.07	5.90	0.02
	TSHT	2.00	7.03	17.64	-	-	-	0.26	6.84	17.64
	Proposed (Voting-TSHT)	2.00	7.01	20.72	2.00	6.91	1.97	0.01	6.30	1.18
	Mode-Finding	2.00	7.03	17.64	-	-	-	0.42	6.96	17.64



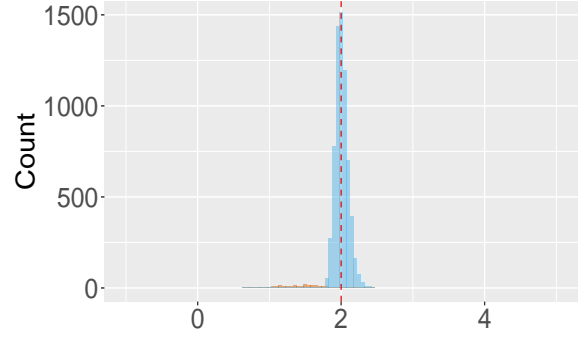
(a) \hat{S}_1



(b) \hat{S}_2 : Remove spurious IVs



(c) \hat{S}_3



(d) \hat{S}_3 (refit)

Figure S2: Plots (a)-(d) correspond to the simulation 2 in Section S4.2. Plots (a)-(c) are histograms of causal effect estimates from valid, invalid and spurious instruments in \hat{S}_1 , \hat{S}_2 and \hat{S}_3 respectively obtained from Algorithm 1 across 1000 Monte Carlo runs. The blue pile represents causal estimates from valid IVs; the green pile refers to invalid IVs; the orange pile is causal estimates from irrelevant variables, including both irrelevant variables from the initial candidate set and pseudo ones. The red dashed line is the true causal effect $\beta^* = 2$. The results are based on $(n, p, \sigma_D^2) = (500, 100, 000, 0)$. The last figure (d) gives the distribution of causal estimates from refitted model.

S4.3 Violation of independence assumption (I3) - simulation 3

In this simulation, to examine the robustness our method, in addition to the violation of no direct effect assumption (I2), we also consider the violation of independence assumption (I3), that is, instrument can be correlated with the unobserved confounding U . Suppose we have 7 relevant instruments, among which one has direct effect on the outcome, one is correlated with U and the others are valid. Instrument Z_2 and U are bivariate normal with correlation 0.6 and variance 1. The other candidates instruments and ϵ_Y are independent standard normal. The variance of random error ϵ_D takes values $\sigma_D^2 = 0, 4$ and the true causal effect β^* is set to 2. The dimension of candidate instruments $p = 100,000$. The true parameters are given as follows.

$$\begin{aligned}\gamma^* &= (2.7, 2.7, 2.7, 2.7, 2.7, 2.7, 2.7, 0, \dots, 0)^T \\ \pi^* &= (3.5, 0, 0, 0, \dots, 0)^T \\ \alpha_D^* &= 4; \alpha_Y^* = -3.\end{aligned}$$

Our comparison includes the proposed method (Proposed), sample splitting (Sample Splitting), two-stage hard thresholding with voting (TSHT) in [Guo et al. \(2018\)](#), the proposed procedure with the voting in [Guo et al. \(2018\)](#) (Proposed (Voting-TSHT)), and the oracle method (Oracle) by assuming that we know the valid instruments a priori. Empirical results are presented in Tables [S5](#) and [S6](#). Histograms of causal effect estimates under $\sigma_D^2 = 0$ are presented in Figure [S3](#).

Table S5: Performance summary for various methods and σ_D^2 under simulation 3 across 1000 Monte Carlo runs with $n = 500$ and $p = 100,000$. We make the numbers bold for the method with the best performance except for the oracle estimate. Standard errors are presented in the bracket if applicable

	Method	Bias $\times 10$ (SE $\times 10$)	RMSE $\times 10$	Coverage (Nominal = 95%)
$\sigma_D^2 = 0$	Proposed	-0.08(0.02)	0.55	0.94
	Sample Splitting	-0.89(0.02)	1.04	0.32
	TSHT	-1.59(0.04)	2.09	0.45
	Proposed (Voting-TSHT)	-0.36(0.03)	0.98	0.90
	Oracle	-0.01(0.01)	0.35	0.96
$\sigma_D^2 = 4$	Proposed	-0.12(0.02)	0.59	0.91
	Sample Splitting	-0.47(0.04)	1.44	0.39
	TSHT	-0.80(0.03)	1.23	0.62
	Proposed (Voting-TSHT)	-0.22(0.02)	0.70	0.90
	Oracle	-0.01(0.01)	0.35	0.95

The simulation results suggest that the proposed method still works even if the independence assumption (I3) is violated. And the undesirable performance of the sample splitting algorithm is due to the fact that in average one invalid instrument is misidentified as valid, as shown in \hat{S}_3 of

Table S6: Average number of invalid, valid IVs and irrelevant variables in $\hat{\mathcal{S}}_1$, $\hat{\mathcal{S}}_2$ and $\hat{\mathcal{S}}_3$ under simulation 3 respectively across 1000 Monte Carlo runs. The results are based on $n = 500$ and $p = 100,000$. “—” stands for “inapplicable”

	Method	$\hat{\mathcal{S}}_1$			$\hat{\mathcal{S}}_2$			$\hat{\mathcal{S}}_3$		
		Invalid	Valid	Irrelevant	Invalid	Valid	Irrelevant	Invalid	Valid	Irrelevant
$\sigma_D^2 = 0$	Proposed	2.00	5.00	6.22	1.99	5.00	1.79	0.00	4.65	0.27
	Sample Splitting	1.99	4.97	6.94	1.97	4.95	1.81	0.97	4.93	0.01
	TSHT	2.00	5.00	3.37	—	—	—	0.01	1.88	3.28
	Proposed (Voting-TSHT)	2.00	5.00	6.22	1.99	5.00	1.79	0.00	3.79	0.70
$\sigma_D^2 = 4$	Proposed	2.00	5.00	10.33	1.38	4.98	1.91	0.02	4.57	0.90
	Sample Splitting	1.99	4.95	12.02	1.75	4.84	1.85	0.86	4.64	0.02
	TSHT	2.00	5.00	3.99	—	—	—	0.22	3.76	3.91
	Proposed (Voting-TSHT)	2.00	5.00	10.33	1.38	4.98	1.91	0.02	4.26	1.20

Table S6.

S4.4 Some irrelevant variables are correlated with valid instruments - simulation 4

In our previous simulations, the irrelevant variables are independent of the relevant ones. To further examine the robustness of our method, in this subsection we consider the scenario where noise variables can be correlated with valid instruments. We set $p = 100,000$. In the simulations, we have 9 relevant instruments generated from independent standard normal, and 2 of them are invalid which have direct effect on the outcome. For each $j = 3, \dots, 7$, we generate 10 irrelevant variables which follow $N(0, 1)$ and are correlated with valid instrument Z_j . In our numerical experiments, we consider weak and moderate correlations, which are 0.2 and 0.6 respectively. All the other irrelevant variables, the unobserved confounding U and random error ϵ_Y are independently generated from $N(0, 1)$. Random error ϵ_D follows $N(0, \sigma_D^2)$ with $\sigma_D^2 = 0, 4, 8$. We set the true causal effect $\beta^* = 2$. The true parameters are set as

$$\begin{aligned}\gamma^* &= (2.5, 2.7, 2.8, -2.9, -3, -3.1, 3.2, 3.3, 3.5, 0, \dots, 0)^T \\ \pi^* &= (-3.5, 3.5, 0, 0, \dots, 0)^T \\ \alpha_D^* &= 4; \alpha_Y^* = -3.\end{aligned}$$

Our comparison includes the proposed method (Proposed), sample splitting (Sample Splitting), two-stage hard thresholding with voting (TSHT) in Guo et al. (2018), the proposed procedure with the voting in Guo et al. (2018) (Proposed (Voting-TSHT)), and the oracle method (Oracle) by assuming that we know the valid instruments a priori. We evaluate the performance in terms of bias, efficiency and validity of inference, and summarize the simulation results in Tables S7 and S8. Histograms of causal effect estimates for weak and moderate correlation are displayed in

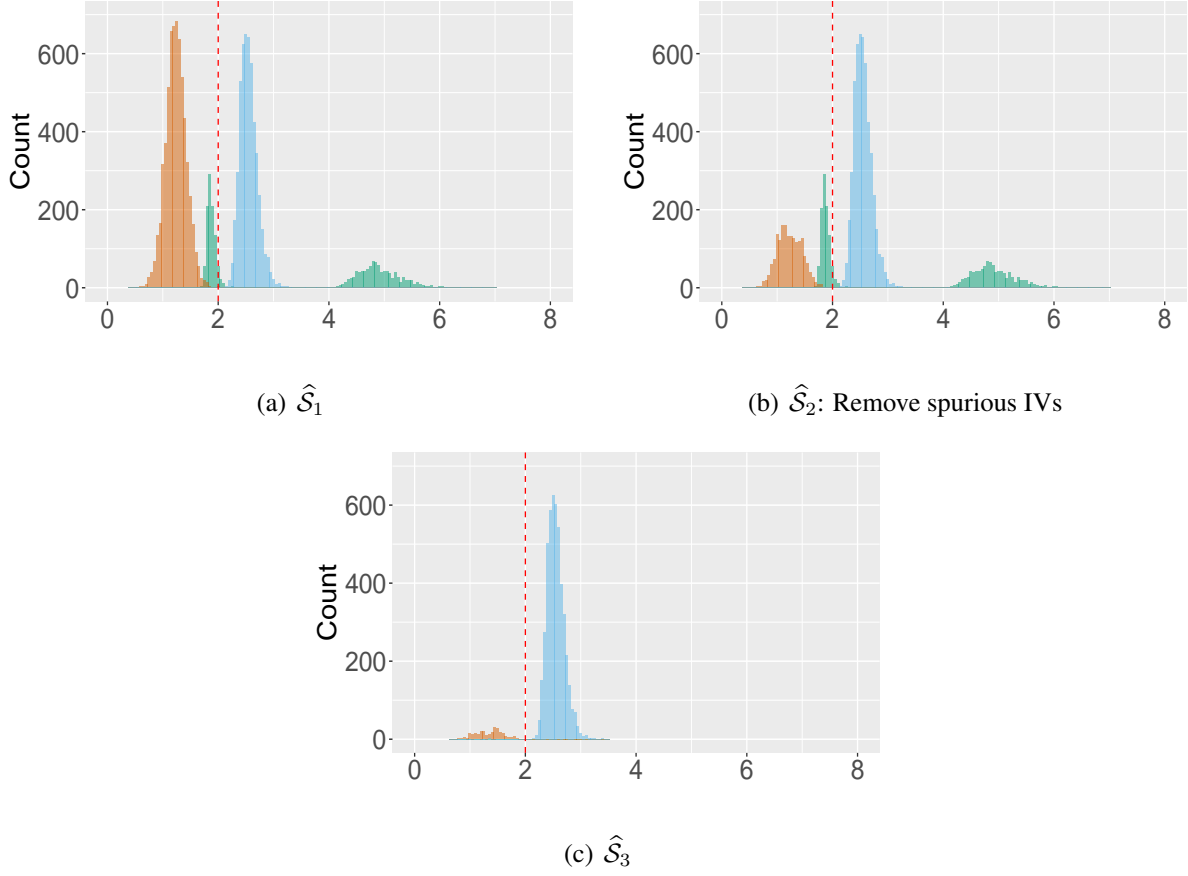


Figure S3: Plots (a)-(c) correspond to the simulation 3 in Section S4.2. Plots (a)-(c) are histograms of causal effect estimates from valid, invalid and spurious instruments in \hat{S}_1 , \hat{S}_2 and \hat{S}_3 respectively obtained from Algorithm 1 across 1000 Monte Carlo runs. The blue pile represents causal estimates from valid IVs; the green pile refers to invalid IVs; the orange pile is causal estimates from irrelevant variables, including both irrelevant variables from the initial candidate set and pseudo ones. The red dashed line is the true causal effect $\beta^* = 2$. The results are based on $(n, p, \sigma_D^2) = (500, 100, 000, 0)$.

Figure S4 and Figure S5 respectively.

Table S7: Performance summary for various methods and σ_D^2 under simulation 4 across 1000 Monte Carlo runs with $n = 500$ and $p = 100,000$. We make the numbers bold for the method with the best performance except the oracle estimate. Standard errors are presented in the bracket if applicable. For $SE < 0.005$, we report as $SE = 0.00$

	Method	Bias $\times 10$ (SE $\times 10$)	RMSE $\times 10$	Coverage (Nominal = 95%)
Weak Correlation				
$\sigma_D^2 = 0$	Proposed	-0.03(0.01)	0.40	0.94
	Sample Splitting	-0.04(0.06)	1.88	0.88
	TSHT	-0.75(0.02)	0.91	0.43
	Proposed (Voting-TSHT)	-0.16(0.02)	0.67	0.93
	Oracle	-0.03(0.01)	0.32	0.94
$\sigma_D^2 = 4$	Proposed	-0.05(0.01)	0.46	0.93
	Sample Splitting	0.04(0.07)	2.13	0.80
	TSHT	-0.48(0.01)	0.57	0.63
	Proposed (Voting-TSHT)	-0.15(0.02)	0.60	0.91
	Oracle	-0.03(0.01)	0.32	0.95
$\sigma_D^2 = 8$	Proposed	-0.02(0.01)	0.41	0.94
	Sample Splitting	0.23(0.07)	2.20	0.74
	TSHT	-0.46(0.01)	0.56	0.63
	Proposed (Voting-TSHT)	-0.08(0.02)	0.49	0.93
	Oracle	-0.03(0.01)	0.32	0.95
Moderate Correlation				
$\sigma_D^2 = 0$	Proposed	-0.01(0.01)	0.44	0.94
	Sample Splitting	0.01(0.05)	1.61	0.88
	TSHT	-0.91(0.02)	1.04	0.38
	Proposed (Voting-TSHT)	-0.17(0.02)	0.67	0.92
	Oracle	-0.03(0.01)	0.32	0.94
$\sigma_D^2 = 4$	Proposed	-0.03(0.01)	0.45	0.94
	Sample Splitting	0.21(0.10)	3.09	0.79
	TSHT	-0.49(0.01)	0.61	0.65
	Proposed (Voting-TSHT)	-0.14(0.02)	0.53	0.92
	Oracle	-0.03(0.01)	0.32	0.95
$\sigma_D^2 = 8$	Proposed	-0.04(0.01)	0.43	0.93
	Sample Splitting	0.22(0.08)	2.51	0.71
	TSHT	-0.41(0.01)	0.51	0.71
	Proposed (Voting-TSHT)	-0.11(0.02)	0.52	0.92
	Oracle	-0.03(0.01)	0.32	0.95

In the presence of irrelevant variables correlated with valid instruments, the proposed method

Table S8: Average number of invalid, valid IVs and irrelevant variables in $\hat{\mathcal{S}}_1$, $\hat{\mathcal{S}}_2$ and $\hat{\mathcal{S}}_3$ under simulation 4 respectively across 1000 Monte Carlo runs. The results are based on $n = 500$ and $p = 100,000$. “–” stands for “inapplicable”

		$\hat{\mathcal{S}}_1$			$\hat{\mathcal{S}}_2$			$\hat{\mathcal{S}}_3$		
Method		Invalid	Valid	Irrelevant	Invalid	Valid	Irrelevant	Invalid	Valid	Irrelevant
Weak Correlation										
$\sigma_D^2 = 0$	Proposed	2.00	7.00	13.07	2.00	7.00	2.01	0.00	6.73	0.23
	Sample Splitting	1.87	6.94	18.88	1.87	6.77	1.93	0.18	6.76	0.04
	TSHT	2.00	7.00	16.45	–	–	–	0.00	5.41	16.45
	Proposed (Voting-TSHT)	2.00	7.00	13.07	2.00	7.00	2.01	0.00	5.97	0.65
$\sigma_D^2 = 4$	Proposed	2.00	7.00	16.95	2.00	7.00	2.12	0.00	6.56	0.43
	Sample Splitting	1.83	6.90	24.29	1.83	6.60	1.79	0.30	6.57	0.04
	TSHT	2.00	7.00	16.91	–	–	–	0.00	6.82	16.91
	Proposed (Voting-TSHT)	2.00	7.00	16.95	2.00	7.00	2.12	0.00	6.12	1.07
$\sigma_D^2 = 8$	Proposed	1.99	7.00	20.45	1.99	6.95	2.07	0.00	6.65	0.80
	Sample Splitting	1.77	6.82	28.89	1.77	6.06	1.88	0.40	5.90	0.07
	TSHT	2.00	7.00	17.78	–	–	–	0.00	6.96	17.78
	Proposed (Voting-TSHT)	1.99	7.00	20.45	1.99	6.95	2.07	0.00	6.27	1.08
Moderate Correlation										
$\sigma_D^2 = 0$	Proposed	2.00	6.98	12.27	2.00	6.98	2.03	0.00	6.43	0.24
	Sample Splitting	1.87	6.79	19.08	1.87	6.65	1.96	0.18	6.63	0.05
	TSHT	2.00	7.00	12.82	–	–	–	0.00	3.87	12.81
	Proposed (Voting-TSHT)	2.00	6.98	12.27	2.00	6.98	2.03	0.00	5.79	0.81
$\sigma_D^2 = 4$	Proposed	2.00	6.90	15.86	2.00	6.89	2.17	0.00	6.28	0.48
	Sample Splitting	1.82	6.57	24.28	1.82	6.30	2.00	0.32	6.24	0.08
	TSHT	2.00	7.00	13.25	–	–	–	0.00	6.18	13.24
	Proposed (Voting-TSHT)	2.00	6.90	15.86	2.00	6.89	2.17	0.00	5.82	1.21
$\sigma_D^2 = 8$	Proposed	1.99	6.68	19.50	1.99	6.58	2.14	0.00	6.20	1.01
	Sample Splitting	1.75	6.29	28.85	1.75	5.60	2.08	0.41	5.32	0.08
	TSHT	2.00	6.99	13.81	–	–	–	0.00	6.79	13.80
	Proposed (Voting-TSHT)	1.99	6.68	19.50	1.99	6.58	2.14	0.00	5.86	1.35

can still correctly identify most valid instruments and thus achieve desired level of coverage. Overall, the proposed procedure is comparable with the oracle estimate.

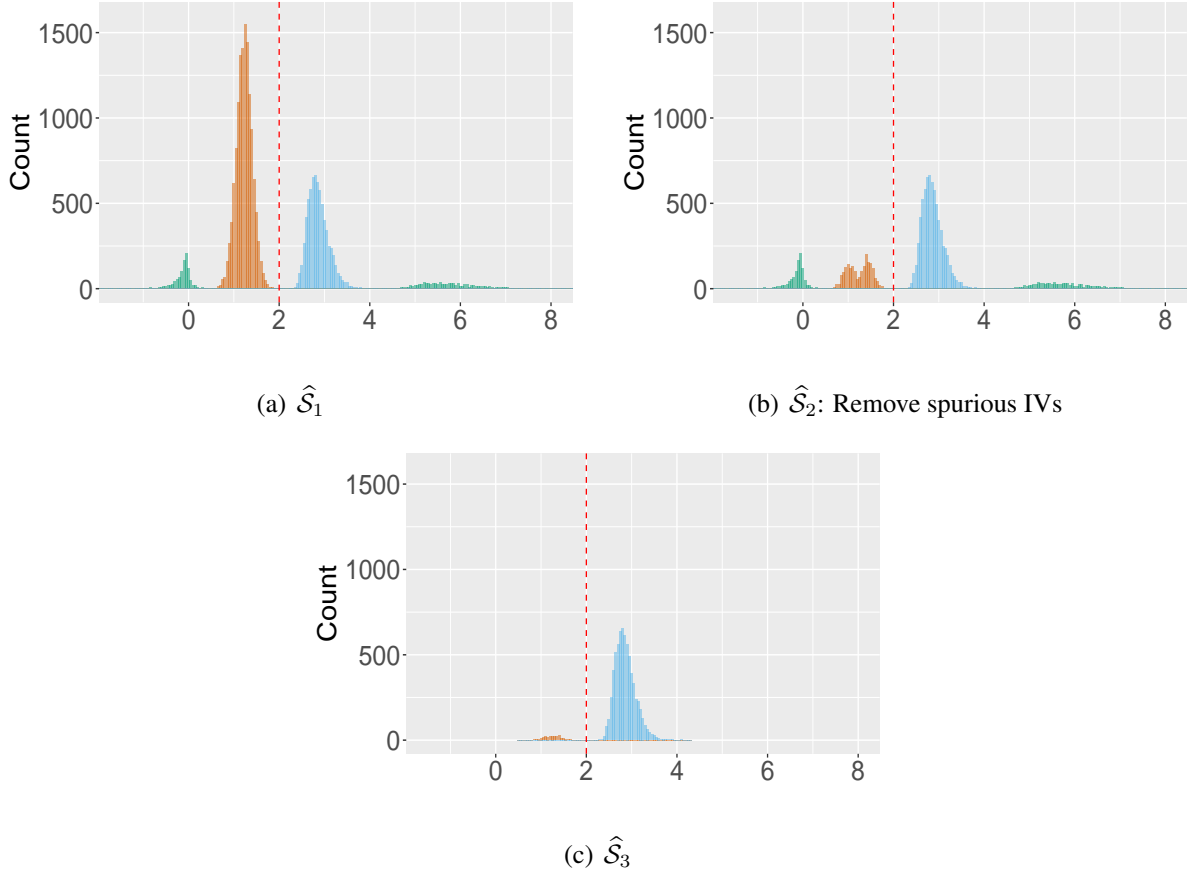


Figure S4: Plots (a)-(c) correspond to the simulation 4 for weak correlation in Section S4.4. Plots (a)-(c) are histograms of causal effect estimates from valid, invalid and spurious instruments in \hat{S}_1 , \hat{S}_2 and \hat{S}_3 respectively obtained from Algorithm 1 across 1000 Monte Carlo runs. The blue pile represents causal estimates from valid IVs; the green pile refers to invalid IVs; the orange pile is causal estimates from irrelevant variables, including both irrelevant variables from the initial candidate set and pseudo ones. The red dashed line is the true causal effect $\beta^* = 2$. The results are based on $(n, p, \sigma_D^2) = (500, 100, 000, 0)$.

S4.5 Competing methods in econometric literature-simulation 5

In this section, we consider some competing approaches which deal with many instruments and allow for weak IVs in the econometric literature to lend further support of our proposed method. Donald & Newey (2001) provided explicit forms for asymptotic mean squared error (MSE) of two-stage least squares (2SLS) and limited-information maximum likelihood (LIML) estimators, which

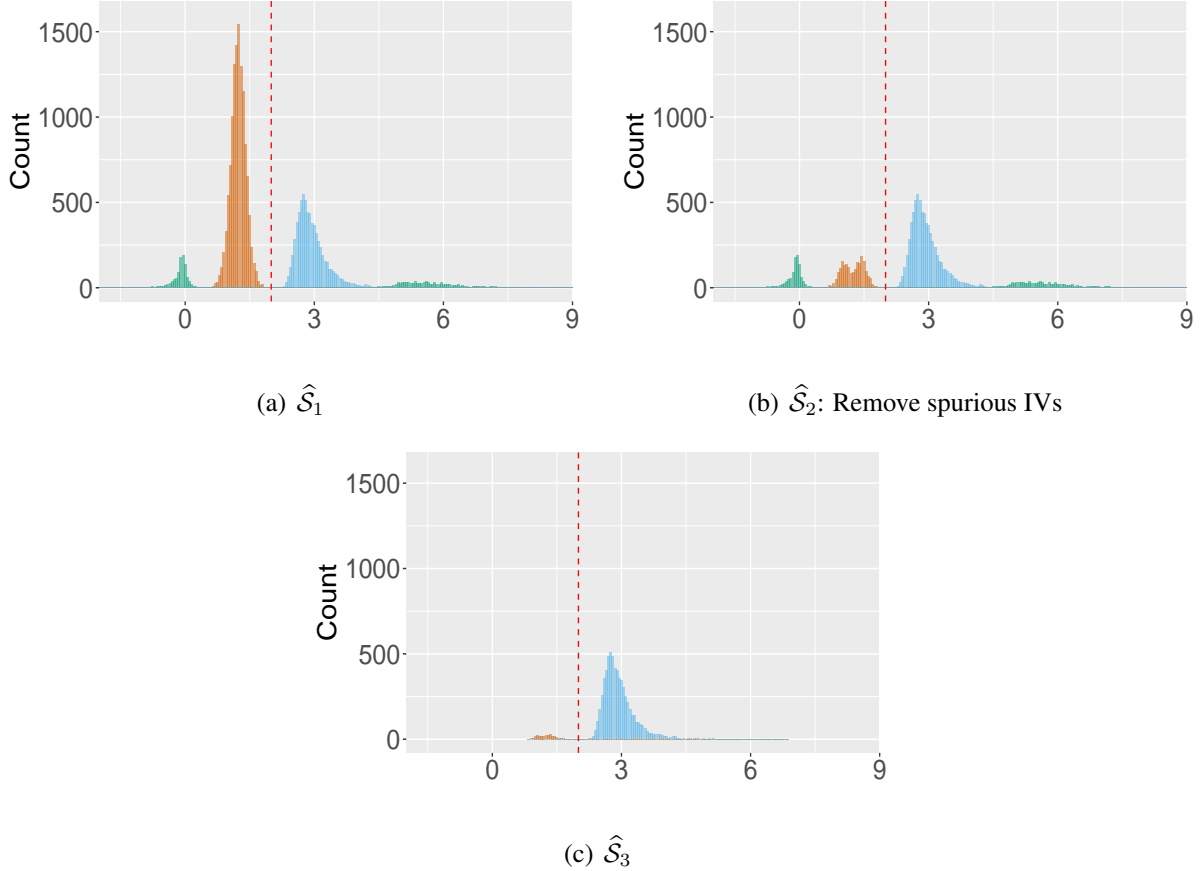


Figure S5: Plots (a)-(c) correspond to the simulation 4 for moderate correlation in Section S4.4. Plots (a)-(c) are histograms of causal effect estimates from valid, invalid and spurious instruments in \hat{S}_1 , \hat{S}_2 and \hat{S}_3 respectively obtained from Algorithm 1 across 1000 Monte Carlo runs. The blue pile represents causal estimates from valid IVs; the green pile refers to invalid IVs; the orange pile is causal estimates from irrelevant variables, including both irrelevant variables from the initial candidate set and pseudo ones. The red dashed line is the true causal effect $\beta^* = 2$. The results are based on $(n, p, \sigma_D^2) = (500, 100, 000, 0)$.

is a function of the number of instruments. They found that selecting the number of instruments by minimizing MSE can improve performance in the presence weak instruments. “D2SLS” and “DLIML” refer to the refined 2SLS and LIML estimators by [Donald & Newey \(2001\)](#) respectively. We also include regularized 2SLS ([Carrasco, 2012](#)) and regularized LIML ([Carrasco & Tchuente, 2015](#)) based on Tikhonov (ridge) regularization, which aim to solve the problem of many instruments efficiently when some are irrelevant. We use the same notation “T2SLS” and “TLIML” as [Carrasco & Tchuente \(2015\)](#) to denote these methods.

In the simulation, we assume no invalid instruments, that is, candidate instrument is either valid or irrelevant. The candidate instruments, the unobserved confounding U , the random error ϵ_Y are independently generated from independent $N(0, 1)$. The random error ϵ_D follows $N(0, \sigma_D^2)$ with $\sigma_D^2 = 0, 4, 8$. The true parameters are set as follows.

$$\begin{aligned}\gamma^* &= (2.5, 2.5, 2.5, 2.5, 2.5, 2.5, 2.5, 0, \dots, 0)^T \\ \pi_j^* &= 0, \text{ for } j = 1, \dots, p \\ \alpha_D^* &= 4; \alpha_Y^* = -3.\end{aligned}$$

Evaluation of the performance is carried out across 1000 Monte Carlo runs. Same as before, we first reduce the dimension of candidate instruments to $s = 500$ via marginal screening and then apply D2SLS, DLIML, T2SLS and TLIML to the selected candidates. We report bias, root-mean-square error (RMSE) and empirical coverage for each method, and the oracle estimate which uses valid instruments only. We summarize the results in Table [S9](#).

In summary, the proposed method performs similarly to the oracle estimate which is served as benchmark. “D2SLS” works well when $\sigma_D^2 = 0$ and perform badly as σ_D^2 increases. “DLIML” seems to overfit under $\sigma_D^2 = 0$. And all the other methods cannot achieve desired performance.

Table S9: Performance summary for the comparison with competing methods in econometric literature-simulation 5. Results are obtained from 1000 Monte Carlo runs with $p = 100,000$. We make the numbers bold for the method with the best performance except the oracle estimate. Standard errors are presented in the bracket if applicable. For $SE < 0.005$, we report as $SE = 0.00$

	Method	Bias $\times 10$ (SE $\times 10$)	RMSE $\times 10$	Coverage (Nominal = 95%)
$\sigma_D^2 = 0$	Proposed	-0.08(0.01)	0.41	0.94
	T2LS	-1.87(0.01)	1.88	0.00
	TLIML	-1.85(0.01)	1.86	0.00
	D2SLS	-0.11(0.01)	0.25	0.90
	DLIML	-0.22(0.01)	0.30	0.98
	Oracle	-0.03(0.01)	0.21	0.95
$\sigma_D^2 = 4$	Proposed	-0.06(0.01)	0.31	0.93
	T2LS	-1.76(0.01)	1.77	0.00
	TLIML	-1.74(0.01)	1.75	0.00
	D2SLS	-0.24(0.01)	0.35	0.72
	DLIML	-0.58(0.01)	0.61	0.49
	Oracle	-0.03(0.01)	0.21	0.95
$\sigma_D^2 = 8$	Proposed	-0.07(0.01)	0.32	0.93
	T2LS	-1.66(0.01)	1.67	0.00
	TLIML	-1.65(0.01)	1.66	0.00
	D2SLS	-0.43(0.01)	0.51	0.44
	DLIML	-0.78(0.01)	0.81	0.12
	Oracle	-0.03(0.01)	0.21	0.95